The calcineurin regulator Sarah enables distinct forms of homeostatic plasticity at the *Drosophila* neuromuscular junction

Noah S. Armstrong[1,2] and C. Andrew Frank[1,2, 3]

[1]Department of Anatomy and Cell Biology, University of Iowa Carver College of Medicine, Iowa City, IA, United States; [2]Interdisciplinary Graduate Program in Neuroscience University of Iowa, Iowa City, IA, United States; [3]Iowa Neuroscience Institute, University of Iowa, Iowa City, IA

*** Correspondence:**

C. Andrew Frank

andy-frank@uiowa.edu

Keywords: *Drosophila melanogaster*, NMJ, neurotransmission, plasticity, synaptic homeostasis, synaptic dysfunction, calcineurin, *sarah* (*sra*)

Abstract

The ability of synapses to maintain physiological levels of evoked neurotransmission is essential for neuronal stability. A variety of perturbations can disrupt neurotransmission, but synapses often compensate for disruptions and work to stabilize activity levels, using forms of homeostatic synaptic plasticity. Presynaptic homeostatic potentiation (PHP) is one such mechanism. PHP is expressed at the *Drosophila melanogaster* larval neuromuscular junction (NMJ) synapse, as well as other NMJs. In PHP, presynaptic neurotransmitter release increases to offset the effects of impairing muscle transmitter receptors. Prior *Drosophila* work has studied PHP using different ways to perturb muscle receptor function: either acutely (using pharmacology) or chronically (using genetics). Some data suggested that cytoplasmic calcium signaling was important for expression of PHP after genetic impairment of glutamate receptors. Here we followed up on that observation. We used a combination of transgenic *Drosophila* RNA interference and overexpression lines, along with NMJ electrophysiology, synapse imaging, and pharmacology to test if regulators of the calcium/calmodulin-dependent protein phosphatase calcineurin are necessary for the normal expression of PHP. We found that either pre- or postsynaptic dysregulation of a *Drosophila* gene regulating calcineurin, *sarah* (*sra*), blocks PHP. Tissue-specific manipulations showed that increases and decreases in *sra* expression are both detrimental to PHP. Additionally, pharmacologically and genetically induced forms of expression of PHP are functionally separable depending entirely upon which *sra* genetic manipulation is used. Surprisingly, dual-tissue pre- and postsynaptic *sra* knockdown or overexpression can ameliorate PHP blocks revealed in single-tissue experiments. Pharmacological and genetic inhibition of calcineurin corroborated this latter finding. Our results suggest tight calcineurin regulation is needed across multiple tissue types to stabilize peripheral synaptic outputs.

INTRODUCTION

Normal synapse function permits a pre-determined physiological range of activity. Challenges to synapse function can force activity beyond setpoint limits. To maintain stability, synaptic and circuit level homeostatic mechanisms exist in vertebrates and invertebrates (Davis, 2006, Marder, 2012, Pozo and Goda, 2010, Frank, 2014a). Defects in homeostatic plasticity can impair the preservation of neuronal activity and may be associated with neurological conditions that display instabilities including ataxia, migraine, schizophrenia, Alzheimer's disease and epilepsy (Andre et al., 2018, Dickman and Wondolowski, 2013, Wondolowski and Dickman, 2013, Bliss et al., 2014). Synaptic homeostasis has also been implicated as being necessary for the manifestation of normal sleep behavior (Tononi and Cirelli, 2006, Kikuma et al., 2019). For these diverse behaviors or neurological disorders, the relevant synaptic activities and functional challenges operate on varying timescales, from minutes (e.g., perturbations that induce migraine) to years (e.g., conditions like Alzheimer's Disease). Yet there are significant gaps in understanding of how neuronal stability is maintained, across neural tissue types and over broad timescales.

We can address some of these gaps using model synapses, like the *Drosophila melanogaster* neuromuscular junction (NMJ). The *Drosophila* NMJ is a well-studied synapse (Menon et al., 2013). It is suitable for combining approaches in genetics, development, and electrophysiology (Jan and Jan, 1976). For homeostatic synaptic plasticity, the NMJ has been key for mechanistic discovery (Frank et al., 2020). One well-characterized form of homeostatic plasticity is called presynaptic homeostatic potentiation (PHP). In *Drosophila*, PHP is initiated when postsynaptic glutamate receptors are impaired, decreasing quantal size. The synapse detects this impairment, and a muscle-to-nerve signaling process drives increased presynaptic glutamate release. The prevailing model is that potentiated release happens after retrograde signaling triggers an increase in presynaptic calcium influx through Ca_V2 voltage-gated calcium channels (Frank et al., 2006, Frank et al., 2009, Müller and Davis, 2012, Wang et al., 2014, Younger et al., 2013). This increase in presynaptic calcium influx coincides with an increased readily releasable pool (RRP) of synaptic vesicles (Harris et al., 2015, Müller et al., 2015, Müller et al., 2012, Weyhersmüller et al., 2011). These modifications drive the ability of the motor neuron to deliver more glutamate to the cleft, offsetting the decreased quantal size.

68 PHP is studied using different kinds of manipulations. Acute inhibition of glutamate
69 receptors causes PHP to be expressed rapidly, in minutes (Frank et al., 2006). By contrast, genetic
70 manipulations last over extended developmental time (Davis et al., 1998, DiAntonio et al., 1999,
71 Petersen et al., 1997). Acute PHP can be induced and expressed by applying glutamate receptor
72 inhibitors, like Philanthotoxin-433 (PhTx) (Frank et al., 2006) or GYKI-53655 (Nair et al., 2021).
73 Alternatively, glutamate receptors can be impaired genetically using a loss of function mutation in
74 *GluRIIA*^{SP16} (Petersen et al., 1997), RNAi-mediated knockdown of *GluRIII* (Brusich et al., 2015), or
75 a variety of other manipulations that impair receptor expression throughout development
76 (reviewed in (Frank, 2014a)). Each of these manipulations results in decreased quantal size, offset
77 by increased quantal content, resulting in normal levels of evoked excitation.

78 In prior work, we reported that a signaling modality including Gq, *Plc21C* (*Drosophila*
79 PLCβ homolog), IP_3 receptors, and ryanodine receptors were necessary for the expression of PHP
80 after genetic glutamate receptor loss, but not after acute pharmacological PhTx challenge (James
81 et al., 2019). IP_3 receptors and ryanodine receptors have dual pre- and postsynaptic functions by
82 mediating the release of intracellular calcium from intracellular calcium stores (Kadamur and Ross,
83 2013, Philip et al., 2010). However, it is unclear which calcium-dependent molecules must be
84 activated or regulated via the release of calcium from intracellular stores to promote homeostatic
85 potentiation.

86 Calcineurin is a well conserved Ca^{2+}/calmodulin-dependent protein phosphatase that is
87 found in most mammalian tissues but is expressed at high levels in the brain, and it has been shown
88 to regulate ion channel function and trafficking, apoptosis, gene regulation, receptor trafficking,
89 neuronal plasticity, and immune processes (Rusnak and Mertz, 2000, Furman and Norris, 2014,
90 Musson and Smit, 2011, Baumgärtel and Mansuy, 2012). Calcineurin is also regulated by a family of
91 proteins known as regulators of calcineurin (RCAN1), which are the product of Down Syndrome
92 Critical Region 1 (DSCR1) gene (Park et al., 2009, Harris et al., 2005). There is evidence that suggests
93 that RCAN family members inhibit calcineurin activity (Kingsbury and Cunningham, 2000, Lee et al.,
94 2003). The *Drosophila* gene *sarah* (*sra*; also known as *nebula*) encodes the only known ortholog
95 of DSCR1 in *Drosophila* (Chang et al., 2003). Sra/Nebula/DSCR1 (herein: Sra) has been shown to
96 physically associate with the catalytic subunit of calcineurin (Takeo et al., 2006). Evidence suggests
97 that Sra inhibits calcineurin, as calcineurin activity has been shown to be approximately 40%

98 higher in *sra* mutants in comparison to controls or heterozygous mutants (Chang et al., 2003). *sra*
99 gene function has been shown to be required for mitochondrial function (Chang and Min, 2005),
100 female meiosis and egg activation (Takeo et al., 2006, Horner et al., 2006, Takeo et al., 2012), sleep
101 regulation (Nakai et al., 2011) and learning (Chang et al., 2003).

102 Here we report that both increases and decreases in *sra* gene expression – in either
103 presynaptic neuron or postsynaptic muscle – result in PHP impairment. Using genetics, we found
104 that different modes of PHP expression were functionally separable, as specific *sra* manipulations
105 compromised expression of PHP triggered by acute pharmacology or chronic genetic mutation.
106 We found that tissue-specific manipulations of *sra* resulted in strong blocks of PHP. But
107 surprisingly, dual tissue manipulations did not. Concurrent pre- and postsynaptic *sra* knockdown
108 or overexpression led to weaker (or no) blocks of PHP compared to single tissue impairments.
109 Consistent with this latter finding, global pharmacological inhibition of calcineurin via FK506
110 increases homeostatic capabilities following a genetic PHP challenge.

111 Taken together, our data highlight a novel idea for homeostasis at the synapse. Proteins
112 like Sra are present in multiple synaptic tissues; if those factors are manipulated in tissue-specific
113 ways, there can be profound defects in overall synapse stability. But conversely, global losses (or
114 gains) of function may escape the most severe phenotypes. Our data set a framework for testing
115 how individual molecules contribute to homeostatic synaptic plasticity from different synaptic
116 tissues.

117

118 **METHODS**

119 ***Drosophila* husbandry and stocks**

120 *Drosophila melanogaster* fruit flies were raised on a standard cornmeal and molasses medium
121 prepared according to the recipe from the Bloomington *Drosophila* Stock Center (BDSC,
122 Bloomington, IN). *Drosophila* husbandry was performed according to standard practices
123 (Greenspan, 2004). Larvae were raised at 25ºC in humidity and light controlled (12 h light: 12 h
124 dark) Percival DR-36VL incubators (Geneva Scientific).

125 w^{1118} (Hazelrigg et al., 1984) was used as a non-transgenic wild type stock. The null
126 *GluRIIA*^{SP16} mutant generated previously (Petersen et al., 1997). The *UAS-GluRIII RNAi* line that
127 was used has been described previously (Brusich et al., 2015). GAL4 drivers that were used included
128 the neuronal drivers *elaV*(*C155*)-*GAL4* (Lin and Goodman, 1994) and *Sca-GAL4* (Budnik et al., 1996)
129 and the postsynaptic driver *BG57-GAL4* (Budnik et al., 1996). The *sra RNAi* line that was used was
130 *TRiP.JF02557* (BDSC:27260) (Shaw and Chang, 2013) and the *sra* overexpression line that was
131 used was *sra*^{EY07182} (BDSC:15991) (Lee et al., 2016). The *sra*^{Mi06435} was used alone (BDSC:42393)
132 and in conjunction with the deficiency line *Df(3R)sbd104* (BDSC:1920). The *CaNB RNAi* line that
133 was used was *TRiP.JF02616* (BDSC:27307) (Shaw and Chang, 2013).

134

135 **Electrophysiology and pharmacology**

136 Wandering third instar larvae were collected and dissected for NMJ analysis. Both control and
137 experimental conditions were performed in parallel using identical conditions. Dissections and
138 recordings were performed in a modified HL3 saline (70 mM NaCl, 5 mM KCl, 5mM HEPES, 10
139 mM $NaHCO_3$, 115 mM sucrose, 4.2 mM trehalose, 0.5 mM $CaCl_2$ (unless otherwise noted), 10
140 mM $MgCl_2$, pH 7.2 (Stewart et al., 1994). Neuromuscular junction sharp electrode recordings were
141 performed on muscles 6/7 of abdominal segments A2, A3, and A4. Miniature excitatory
142 postsynaptic potentials (mEPSPs) and excitatory postsynaptic potentials (EPSPs) were conducted
143 as previously described (Brusich et al., 2015, Spring et al., 2016, Yeates et al., 2017, James et al., 2019,
144 Mallik and Frank, 2022).

145 Uncorrected quantal content was calculated per NMJ by dividing the average EPSP by the
146 average mEPSP. Quantal content was then corrected for non-linear summation (NLS quantal
147 content) using the following calculation (McLachlan and Martin, 1981):

148 $$\bar{v}' = E \ln \frac{E}{(E - \bar{v})}$$

149 $\bar{v}'$ is the NLS corrected EPSP, E is the electromotive force (in this case equal to resting membrane
150 potential), and $\bar{v}$ is equal to the EPSP amplitude. To find NLS corrected quantal content, the
151 corrected EPSP amplitude ($\bar{v}'$) is then divided by mEPSP amplitude.

152 Recordings were performed on a Leica microscope using a 10x objective and acquired
153 using an Axoclamp 900A amplifier, Digidata 1440A acquisition system and pClamp10.7
154 (Molecular Devices) software. Data were analyzed using MiniAnalysis (Synaptosoft) and the
155 Clampfit (Molecular Devices) programs. To generate mEPSP and EPSP traces for figures, (x,y)
156 coordinates were pulled from the Clampfit program and imported into GraphPad Prism
157 (GraphPad) software. All traces display the recording that was at or closest to the calculated
158 average of each specific condition.

159 Pharmacological agents were bath applied in recording saline at the final concentrations
160 indicated in the text and figures. The agents included Philanthotoxin-433 (PhTx, Sigma-Aldrich),
161 Cyclosporin A (Sigma-Aldrich), and FK506 (InvivoGen).

162

163 **Immunostaining and analyses**

164 Wandering third instar larvae were dissected on a sylgard Petri plate in HL3 and fixed using
165 Bouin's fixative for 10 minutes or 4% paraformaldehyde in PBS for 30 minutes. Larvae were
166 washed with PBS containing 0.2% Triton X-100 (PBST) for 40 min, blocked for an hour with
167 2.5% BSA, and incubated overnight with primary antibodies at 4ºC. This was followed with
168 another 40 min of washes, and incubation in secondary antibodies for 1.5 hr at room temperature.
169 The primary antibodies used were mouse anti-Synapsin (anti-Syn; 3C11) 1:50 (Developmental
170 Studies Hybridoma Bank, Iowa City, IA); rabbit anti-Dlg 1:15,000 (Budnik et al., 1996); mouse
171 anti-phosphorylated CaMKII (pCaMKII) 1:100 (MA1-047; Invitrogen); rabbit anti-GluRIII 1:150
172 (Marrus et al., 2004, Goel and Dickman, 2018). The following fluorophore conjugated secondary
173 antibodies were also used (Jackson ImmunoResearch Laboratories): goat anti-mouse 488 1:1000
174 (DyLight) and goat anti–rabbit 549 1:2000 (DyLight). Larval preparations were mounted in
175 Vectashield (Vector Laboratories) and imaged at room temperature with a 700 Carl Zeiss laser
176 scanning confocal microscope equipped with 63 × /1.4 NA oil immersion objective using separate
177 channels with four laser lines (405, 488, 555, and 639 nm). All quantifications were performed on
178 muscle 6/7 segments A2 and A3. For NMJ growth analysis, anti-Dlg boutons were counted in
179 muscle after verifying that there was a corresponding cluster of anti-Syn staining in motor neurons.
180 For pCaMKII and GluRIII intensity measurements, a mask was created around the GluRIII
181 channel to define the postsynaptic region and eliminate background. Only pCaMKII signals within

182 this mask at Ib postsynaptic densities were quantified. Images were prepared for publication using
183 Adobe Illustrator.

184

185 **Statistical analyses**

186 Statistical significance was tested using either a Student's T-Test to compare one experimental
187 data set directly to a control data set or using a one-way ANOVA with a Tukey's post-hoc test if
188 multiple data sets were being compared. Specific *p*-value ranges used were as follows: **p*<0.05,
189 ***p*<0.01, and ****p*<0.001. All statistical analyses were conducted using GraphPad Prism
190 software. Data were plotted in GraphPad Prism and final figures were compiled using Adobe
191 Illustrator.

192

193 **RESULTS**

194 **Concurrent neuron and muscle *sra* knockdown do not block PHP**

195 PHP is commonly assessed at the *Drosophila* NMJ using acute Philanthotoxin-433 (PhTx)
196 application to test the rapid expression of PHP (Frank et al., 2006) or $GluRIIA^{SP16}$, the genetic null
197 mutation used to test the expression of PHP throughout life (Petersen et al., 1997). Both
198 manipulations result in decreased mEPSP amplitude while quantal content (corrected for non-
199 linear summation, herein NLS quantal content) increases. This indicates PHP mechanisms working
200 to sustain evoked potentials near normal levels. Given our prior data suggesting that dysregulation
201 of calcium stores disrupted the maintenance of PHP after genetic challenge (Brusich et al., 2015,
202 James et al., 2019), we wanted to test whether combined pre- and postsynaptic *sra* loss-of-function
203 conditions impaired PHP. To do this, we used a *Drosophila* line that contains both neuron and
204 muscle GAL4 drivers to knockdown *sra* using RNAi and applied 20μM PhTx to test rapid PHP
205 expression. This particular *sra RNAi* line been shown to knockdown protein levels of Sarah (also
206 known as Nebula) by about 60% (Shaw and Chang, 2013).

207 PhTx application decreased mEPSP amplitude for both driver control and *sra RNAi*
208 conditions (**Figure 1A**) (Frank et al., 2006). Evoked potentials were maintained for the driver
209 control (**Figure 1B**) because of the compensatory significant increase in NLS quantal content

210 (**Figure 1C**). Dual tissue knockdown of *sra* resulted in a mild decrease in evoked potentials
211 following PhTx incubation. This might be consistent with a small defect in homeostatic plasticity,
212 but there was still a significant increase in NLS quantal content compared to non-drugged controls
213 (**Figure 1A-D** and **Supplementary Table 1**). At a minimum, this indicated partially intact acute
214 PHP expression.

215 To test for the maintenance of PHP, we first used a *Drosophila* line that contains both
216 neuron and muscle GAL4 drivers, along with *UAS-GluRIII RNAi* to provide a genetic homeostatic
217 challenge (Brusich et al., 2015). This *UAS-GluRIII RNAi* reagent is a good first-pass or screening
218 tool to identify genes needed for the maintenance of PHP (Brusich et al., 2015). Again, while there
219 were significant decreases in evoked amplitude in *sra RNAi* synapses challenged with either PhTx
220 or *GluRIII RNAi*, there were still some compensatory increases in NLS quantal content (Figure
221 1A-D). Our interpretation of these data is that PHP mechanisms are partially (or largely) intact
222 when *sra* function is knocked down.

223

224 **Concurrent neuron and muscle *sra* overexpression do not block PHP**

225 We acquired reagents to test if simultaneous pre- and postsynaptic overexpression of *sra* resulted
226 in impairment in forms of PHP. We used the $sra^{EY07182}$ allele. This is a 5' P-element insertion allele
227 in the endogenous *sra* locus with *UAS* binding sites for GAL4 transcriptional control upstream of
228 the *sra* gene; this allows for conditional tissue specific overexpression of *sra*. Overexpression of
229 *sra* neuronally using the pan neuronal driver, *elaV*, and $sra^{EY07182}$ has been shown to result in
230 transcript levels that were approximately twofold higher than controls (Lee et al., 2016).

231 For our electrophysiological experiments, there was a decrease in the EPSPs of neuron +
232 muscle GAL4 >> $sra^{EY07182}$ ("*sra* OE" - overexpression) + *GluRIII RNAi* synapses compared to
233 neuron + muscle GAL4 >> $sra^{EY07182}$ alone, but there was also a significant increase in NLS quantal
234 content (**Figure 1E-H** and **Supplementary Table 1**). Our interpretation of those data is that the
235 chronic expression of PHP is partially (or mostly) intact. Additionally, we there was no significant
236 difference in the EPSPs of neuron + muscle GAL4 >> $sra^{EY07182}$ overexpression animals alone or
237 genetically identical overexpression animals challenged with PhTx (**Figure 1E-H**). Taken as a
238 whole, concurrent overexpression of *sra* both pre-and postsynaptically does not appear to block

homeostatic responses at the NMJ. If anything, phenotypes are subtle, indicating partial impairments of PHP.

Global *sra* mutant has intact PHP but deficient neurotransmission at low calcium

We turned to mutant *Drosophila* stocks to examine loss-of-function alleles. We used the $sra^{Mi06435}$ transposon insertion to test if a global disruption of *sra* function would block PHP or show defective neurotransmission. We compared $sra^{Mi06435}$ alone to wild type and $sra^{Mi06435}$ over chromosomal deficiency. We found no significant differences in EPSP amplitude or NLS quantal content between any groups (**Figure 2A-C** and **Supplementary Table 2)**. To challenge synapses, we used the $GluRIIA^{SP16}$ null mutants that show robust PHP (Petersen et al., 1997). We found a significant decrease in mEPSP amplitude compared to wild type but failed to see a compensatory increase in NLS quantal content. Yet despite this lack of increase in release, we could not conclude that PHP was impaired because there was no significant decrease in EPSP amplitude.

Because mutants showing intermediate PHP phenotypes can be sensitive to levels of calcium (Frank, 2014a, Frank, 2014b, Genç and Davis, 2019), we also tested $sra^{Mi06435}$ and $sra^{Mi06435}/Df$ for defective neurotransmission in low calcium conditions (0.20mM). $sra^{Mi06435}$ and $sra^{Mi06435}/Df$ showed decreased mEPSP amplitude and EPSP amplitude compared to wild type (**Figure 2E-G**). Our $sra^{Mi06435}$ and $sra^{Mi06435}/Df$ data leads us to the interpretation that PHP is mostly intact following global impairment of *sra*, but NMJ function is sensitive to low levels of calcium. This is a phenotype shared with some other homeostatic factors that govern presynaptic release (Frank, 2014b, Frank et al., 2006, Yeates and Frank, 2021).

Postsynaptic *sra* knockdown impairs the rapid expression of PHP but not its maintenance

After testing for dual-tissue functions for *sra* in PHP, we conducted single-tissue experiments. First, we used the *UAS-sra RNAi* transgene to knockdown *sra* expression in the muscle. We applied PhTx to animals that expressed *UAS-sra RNAi* in the muscle using the GAL4 driver, *BG57-GAL4*. Surprisingly, in contrast to the dual-tissue knockdown, postsynaptic knockdown of *sra* completely blocked the rapid expression of PHP, resulting in significantly decreased EPSP amplitudes and a

267 failure to show a compensatory increase in NLS quantal content (**Figure 3B,C** and
268 **Supplementary Table 3**). We tested the if the postsynaptic knockdown of *sra* would also block
269 of the chronic maintenance and expression of PHP. Knockdown of *sra* postsynaptically in a
270 *GluRIIA*^{SP16} background not only exhibited an expected decrease in mEPSP amplitude compared
271 to non-*GluRIIA*^{SP16} controls, but also a marked decrease in EPSP amplitude (**Figure 3E,F** and
272 **Supplementary Table 3**). There was a slight but significant increase in quantal content, which
273 indicates partially intact PHP mechanisms (**Figure 3G**).

274 Our results are consistent with the idea that the knockdown of *sra* postsynaptically induces
275 a complete block when acutely challenged with pharmacology, but only a partial block when
276 chronically challenged genetically. This suggests that the postsynaptic expression of *sra* may have
277 a differential role in regulating two separable forms of PHP. We tested this idea further.

278

279 **Postsynaptic *sra* overexpression blocks the maintenance of PHP but not acute expression**

280 After examining postsynaptic *sra* knockdown, we did the opposite genetic perturbation: we
281 examined overexpression of *sra* postsynaptically. We found that applying PhTx to synapses with
282 *sra* overexpressed postsynaptically reveals partially impaired rapid PHP expression (**Figure 4A-**
283 **D** and **Supplementary Table 4**). There was no significant difference in EPSPs between
284 unchallenged and challenged NMJs. There was a small numerical increase in NLS quantal content,
285 but this increase did not achieve statistical significance (**Figure 4C**).

286 Next, we tested if postsynaptic overexpression of *sra* could block chronic expression of
287 PHP using the *sra*^{EY07182} allele in a *GluRIIA*^{SP16} background. Overexpression of *sra*
288 postsynaptically yielded normal baseline EPSP amplitude (as in Figure 1), but this postsynaptic
289 overexpression of *sra* in *GluRIIA*^{SP16} null NMJ background triggered a significant decrease in
290 EPSP amplitude along with a failure to increase NLS quantal content when compared to the
291 unchallenged control (**Figure 4E-H** and **Supplementary Table 4**). In fact, the NLS quantal
292 content was also significantly decreased in the *GluRIIA*^{SP16} background, which is not a common
293 phenotype. This is indicative a strong block of chronically expressed PHP. Taken together, our
294 data suggest that proper postsynaptic expression of *sra* is critical for the NMJ to respond to
295 different kinds of PHP challenge.

296

297 **Postsynaptic *sra* overexpression does not impair synapse development**

298 Since the postsynaptic overexpression phenotype was the strongest, we checked if it
299 correlated with NMJ developmental defects. In principle, synaptic developmental defects could
300 explain the physiological phenotypes. We immunostained third instar larval *Drosophila* NMJs for
301 presynaptic boutons to quantify their elaboration. We overexpressed *sra* postsynaptically alone
302 and or in conjunction with $GluRIIA^{SP16}$. We visualized NMJ bouton development in synapse 6/7
303 muscle segments A2 and A3 by co-staining with anti-Synapsin (Syn, presynaptic vesicle marker)
304 and anti-Discs Large (DLG, postsynaptic density marker).

305 We did not find marked differences in bouton number between any group for NMJ 6/7
306 within segment A2 or segment A3 (**Figure 5A-G** and **Supplementary Table 5**) (segments
307 analyzed separately due to documented differences in development). We quantified bouton
308 normalized per muscle area and found that postsynaptic overexpression of *sra* resulted in a
309 significant increase compared to other genotypes (**Figure 5H** and **Supplementary Table 5**). This
310 indicates that *sra* overexpression in the muscle may result in smaller muscles – but in any case,
311 these unchallenged animals had intact physiology (**Figure 4**). These data indicate that postsynaptic
312 overexpression of *sra* does not impair gross NMJ development, and therefore, a developmental
313 defect unlikely to be contributing towards the observed PHP block by electrophysiology. The
314 caveat to this experiment is that more subtle developmental changes are possible on the level of
315 active zones or glutamate receptor clusters. We decided to examine a marker known to correlate
316 with PHP expression at a specific motor terminal.

317

318 **Overexpression of *sra* postsynaptically disrupts pCaMKII downregulation in Ib motor**
319 **neurons**

320 To try to gain more mechanistic understanding of how postsynaptic *sra* overexpression may be
321 blocking the maintenance of PHP, we measured phosphorylated CaMKII (pCaMKII) levels and
322 glutamate receptor signal intensity. Genetic glutamate receptor challenges normally result in
323 decreased levels of pCaMKII immunofluorescence (Kikuma et al., 2019, Goel et al., 2017, Li et al.,
324 2018, Newman et al., 2017), and this decrease correlates with successful expression of PHP.

325 We measured pCaMKII intensity at Ib postsynaptic densities. We found a significant
326 decrease in *GluRIIA*^{SP16} animals compared to wild-type animals as has been shown previously
327 (**Figure 6A,B** and **Supplementary Table 6**). Surprisingly, when comparing overexpression of *sra*
328 postsynaptically to overexpression of *sra* postsynaptically in *GluRIIA*^{SP16} null NMJs, we not only
329 failed to see a decrease in pCaMKII intensity, but we saw a significant increase (**Figure 6A,B**).
330 Moreover, when examining GluRIII (also known as GluRIIC) intensity, we saw no significant
331 difference between wild type and *GluRIIA*^{SP16} (**Figure 6A,C**). However, we saw a significant
332 increase in GluRIII intensity in *sra* postsynaptic overexpression in the *GluRIIA*^{SP16} null
333 background when compared to *sra* overexpression alone or wild type (**Figure 6A,C**). Collectively,
334 these data suggest that postsynaptic expression of *sra* is necessary for the downregulation of
335 pCaMKII that results from glutamate receptor perturbation. As a result, it is possible that the
336 synapse (unsuccessfully) attempted to compensate for this by trafficking in more glutamate
337 receptors.

338

339 **Knockdown of *sra* presynaptically impedes the maintenance of PHP but not acute expression**

340 Because we saw strong tissue-specific phenotypes when genetically dysregulating *sra* in the
341 muscle, we tested if knockdown of *sra* presynaptically also affected PHP. Acute application of
342 PhTx to NMJs with *sra* neuronal knockdown did not block Acute PHP expression as EPSP
343 amplitudes were mostly maintained, and NLS quantal content was significantly increased between
344 challenged and unchallenged animals (**Figure 7A-D** and **Supplementary Table 7**).

345 To understand if decreasing *sra* expression presynaptically blocks the long-term expression
346 of PHP, we turned to the *GluRIIA*^{SP16} null mutant again. We found that decreased *sra* expression
347 neuronally blocked chronic PHP because of decreased EPSP amplitude in *GluRIIA*^{SP16}, *sra RNAi*
348 NMJs when compared to *GluRIIA*^{SP16} or *sra RNAi* alone (**Figure 7E-H** and **Supplementary Table**
349 **7**). The *GluRIIA*^{SP16}, *sra RNAi* synapses also failed to show a significant increase in NLS quantal
350 content compared to the unchallenged control (**Figure 7G**). This provides us with evidence that
351 the knockdown of *sra* presynaptically blocks the long-term maintenance phase of PHP

352

353 **Overexpression of *sra* presynaptically blocks long-term PHP expression**

354 Finally, we tested if the presynaptic overexpression of *sra* affects PHP. After applying PhTx to
355 NMJs with *sra* neuronal overexpression, we did not find any significant differences in evoked
356 amplitude while getting a robust increase in NLS quantal content (**Figure 8A-D** and
357 **Supplementary Table 8**). But when we tested chronic PHP expression following neuronal *sra*
358 overexpression, we found impairment. There was a statistically significant decrease in the evoked
359 amplitudes of $sra^{EY07182}$ synapses and a non-significant NLS quantal content increase (**Figure 8E-**
360 **H** and **Supplementary Table 8**). These data are difficult to attribute to sra overexpression alone:
361 we note that the neuronal driver in this experiment also seemed to contribute to the phenotype
362 **(Figure 8F-H)**. From prior work, we know that homozygous $GluRIIA^{SP16}$ null mutant NMJs do
363 not consistently sustain evoked amplitudes perfectly but they do consistently show a robust
364 increase in NLS quantal content (Brusich et al., 2015, Frank et al., 2006, Spring et al., 2016, Yeates et
365 al., 2017, James et al., 2019, Frank et al., 2009).

366 Taking all single-tissue electrophysiology together, our data suggest that changes in the
367 expression of *sra* presynaptically blocks chronic PHP either strongly following *sra RNAi* or weakly
368 following *sra* OE, while the rapid expression of PHP remains unaffected in both contexts. This
369 provides evidence that *sra* has roles both pre- and postsynaptically to allow PHP to function
370 normally. Additionally, the data discussed provide a compelling argument that the acute
371 expression and chronic phases of PHP are functionally separable and do not completely overlap.

372

373 **FK506 reverses the effects of postsynaptic overexpression of *sra***

374 We were puzzled why the single-tissue genetic manipulations of *sra* yielded stronger PHP
375 inhibition. One possibility is that for instances where a molecule normally functions in multiple
376 tissues, synapses could engage homeostatic systems to cope with a global loss (e.g., endogenous
377 genetic mutation) of that molecule. In principle, challenging a synapse with single tissue genetic
378 manipulation could disrupt this process.

379 Our earlier experiments showed a strong chronic PHP block when *sra* was overexpressed
380 postsynaptically (**Figure 4E-H** and **Supplementary Table 4**). Sra is a calcineurin inhibitor. Thus,
381 overexpressing the *sra* gene (*sra* OE) postsynaptically should decrease calcineurin activity in

382 muscle. If the above model is correct, then impairing calcineurin globally via a pharmacological
383 calcineurin inhibitor could reverse the chronic PHP block.

384 FK506 (tacrolimus) is a calcineurin inhibiting drug that binds to FK-binding protein 1 (Liu
385 et al., 1991, Sigal and Dumont, 1992, Clardy, 1995). This immunophilin-drug binds to calcineurin and
386 inhibits its protein phosphatase activity (Kuromi et al., 1997, Clardy, 1995, Swanson et al., 1992). There
387 are notable phenotypes at synaptic preparations. For whole-cell patch clamp in rat cortex,
388 application of FK506 increased the frequency of spontaneous events (Victor et al., 1995). And
389 application of FK506 to *Drosophila* larval neuromuscular junctions has been reported to increase
390 the endocytosis of synaptic vesicles, while having no effect on the frequency of spontaneous events
391 or the mean amplitude of evoked events (Kuromi et al., 1997), though the specificity of FK506 in
392 impairing calcineurin at the *Drosophila* NMJ has not been thoroughly documented.

393 We repeated the experiment of overexpressing *sra* in the muscle, this time incubating NMJ
394 preps with FK506. Larval preps were incubated with 50μM FK506 for 15 minutes prior to
395 electrophysiological recordings. We replicated our earlier finding that *sra* muscle overexpression
396 challenged with the $GluRIIA^{SP16}$ null mutation showed decreased evoked amplitude and a failure
397 to increase NLS quantal content (**Figure 9B,C** and **Supplementary Table 9**). However, when
398 genetically identical animals were incubated with FK506, we found that EPSP amplitude is
399 significantly increased compared to non-drugged controls, and this is a result of increased NLS
400 quantal content (**Figure 9A-D** and **Supplementary Table 9**). Incubation of FK506 did not
401 completely restore EPSPs to wild-type levels, but this experiment suggests that global inhibition
402 of calcineurin across tissues can mitigate the chronic PHP block caused by single-tissue *sra*
403 manipulation. Alternatively, our results may point toward non-specific potentiation
404 presynaptically, induced by FK506. We conducted further tests.

405

406 **FK506 reverses the effects of presynaptic knockdown of *sra***

407 We wondered if we could reverse other PHP defects by pharmacologically blocking calcineurin.
408 We saw a block in chronic PHP following *sra* knockdown presynaptically (**Figure 7E-H**). We
409 repeated this experiment while also including synapses incubated with FK506. As before, in the
410 drug-free condition, EPSP amplitudes were deficient following *sra* presynaptic knockdown

411 challenged via *GluRIIA*^{SP16} and failed to increase NLS quantal content (**Figure 10B,C**). However,
412 incubation with FK506 significantly increased EPSP amplitude in these animals, and this was
413 accompanied by a robust increase in NLS quantal content (**Figure 10A-D** and **Supplementary**
414 **Table 10**). This provides further support that inhibition of calcineurin in a non-tissue-specific
415 pharmacological manner can reverse defects resulting from single tissue *sra* impairments and
416 restore PHP.

417

418 **Pharmacological inhibition of calcineurin generally improves homeostatic capabilities in**
419 **response to chronic PHP challenge**

420 We next tested if the pharmacological inhibition of calcineurin alone would also block PHP. We
421 applied FK506 to *GluRIIA*^{SP16} animals at either 10µM or 50µM concentrations. We saw no change
422 in EPSP amplitude in wild-type animals with drug application at either concentration, but
423 interestingly, in *GluRIIA*^{SP16} animals, we saw an increase in EPSP amplitude and NLS quantal
424 content following 50µM FK506 incubation compared to non-drugged controls (**Figure 11B** and
425 **Supplementary Table 11**). The 50µM concentration also produced increases in mEPSP frequency
426 in both wild type and *GluRIIA*^{SP16} animals (**Figure 11D** and **Supplementary Table 11**). These
427 data are consistent with our hypothesis that global inhibition of calcineurin may create scenarios
428 at the NMJ that are favorable to the expression of PHP.

429 We tested if FK506 increases release probability on its own. To do this, we conducted a
430 failure analysis in very low calcium (0.10mM) (Frank et al., 2006, Petersen et al., 1997). In extremely
431 low calcium, many presynaptic events fail to release vesicles and therefore fail to generate an
432 EPSP. In these low calcium conditions, probability of vesicle release is low (Del Castillo and Katz,
433 1954). Our failure analysis on wild-type and *GluRIIA*^{SP16} animals with and without FK506
434 incubation showed that FK506 significantly decreases the number of failures compared to non-
435 drugged controls (**Figure 11E** and **Supplementary Table 11**). Additionally, successful evoked
436 events were significantly bigger in amplitude (on average) after FK506 incubation compared to
437 non-drugged controls (**Figure 11F**). Taken together, these data suggest that FK506 increases
438 release probability. This may be occurring because of calcineurin inhibition increasing presynaptic
439 calcium either via influx from voltage-gated channels or efflux via intracellular stores.

440 As shown in our failure analysis experiment, FK506 can increase the EPSP amplitude in
441 wild-type animals in low calcium (**Figure 11F** and **Supplementary Table 11**). While there were
442 no changes at our standard calcium concentration of 0.5mM (**Figure 11B**), it is possible that at our
443 standard calcium concentration, we are having a "ceiling effect" where the application of FK506
444 may not be able to increase the EPSPs any further due to electromotive driving forces. To test this
445 idea, we conducted an experiment in 0.20mM Ca^{2+} in both wild type and *GluRIIA*^{SP16} animals with
446 and without FK506. As we predicted, the lower calcium concentration allowed us to detect an
447 increase in evoked amplitude and NLS quantal content in both genotypes following incubation
448 with FK506 (**Figure 11H,I** and **Supplementary Table 11**). This supports the idea that
449 pharmacological calcineurin inhibition may be potentiating calcium levels to increase release
450 probability.

451

452 **Postsynaptic knockdown of the calcineurin encoding gene *CaNB* blocks PHP maintenance**

453 Finally, we wanted to test if knockdown of a calcineurin subunit led to similar blocks in PHP as
454 observed with our *sra* manipulations. In *Drosophila*, there are three genes that encode the catalytic
455 subunit, CN A (*CaNA1*, *Pp2B-14D*, and *CaNA-14F*) and two genes that encode the regulatory
456 subunit, CN B (*CaNB* and *CaNB2*) (Takeo et al., 2006). *CaNA1*4-*F* and *Pp2B-14D* share 82%
457 protein sequence identity and share approximately 62% identity with *CaNA1*, while *CaNB* and
458 *CaNB2* share 98% similarity in protein sequence (Tomita et al., 2011). Presynaptic knockdown of
459 *CaNB* leads to increased frequency of ectopic neuromuscular contacts, and *CaNB* knockouts have
460 been shown to have significantly reduced sleep (Nakai et al., 2011, Vonhoff and Keshishian, 2017).
461 Knockdown of *CaNB* reduces calcineurin activity, similar to *sra* overexpression (Lee et al., 2016,
462 Shaw and Chang, 2013).

463 We first tested whether combined pre- and postsynaptic *CaNB* conditions impaired PHP,
464 like how we tested *sra* overexpression conditions (**Figure 1**). Dual tissue knockdown of *CaNB*
465 resulted in a mild decrease in evoked potentials following PhTx incubation, and there was a slight
466 but insignificant increase in NLS quantal content (**Figure 12A-C** and **Supplementary Table 12**).
467 When testing the maintenance of PHP using *UAS-GluRIII RNAi*, dual tissue knockdown of *CaNB*
468 did not impair evoked potentials and showed a robust increase in NLS quantal content. Taken

469 together, these data suggest a weak effect of *CaNB* dual tissue knockdown on acute PHP
470 expression and no effect on long-term PHP maintenance.

471 Based on our earlier experiments that showed a strong block in the maintenance of PHP
472 following overexpression of *sra* postsynaptically (**Figure 4E-G**), we wanted to test if the
473 knockdown of *CaNB* specifically in muscle showed a similar block. Knockdown of *CaNB*
474 postsynaptically in conjunction with *UAS-GluRIII RNAi* resulted in decreased EPSP amplitude and
475 a failure to increase NLS quantal content (**Figure 12E-G** and **Supplementary Table 12**). We also
476 applied PhTx to synapses with *CaNB* overexpressed postsynaptically and found no significant
477 difference in EPSPs between challenged and unchallenged NMJs, along with a robust increase in
478 NLS quantal content (**Figure 12E-G**). These results suggest that a reduction in calcineurin activity
479 postsynaptically impairs chronic expression of PHP while leaving acute expression intact.

480

481 **DISCUSSION**

482 In this study, we provide a new framework for understanding how individual proteins from
483 different synaptic tissues contribute to Presynaptic Homeostatic Potentiation (PHP). This work
484 offers a new way to consider how overall synaptic stability is maintained through different kinds
485 of challenges to synapse function.

486 We show that concurrent neuronal and muscle knockdown or overexpression of *sra,* a
487 gene encoding a calcineurin regulator, does not strongly impair synaptic homeostatic
488 compensation mechanisms (**Figure 1**). Global genetic mutation of *sra* does not impair them either,
489 but it does reveal that (like homeostatically challenged synapses) the mutant synapse is quite
490 sensitive to low levels of extracellular calcium (**Figure 2**). Impairing *sra* in a tissue-specific
491 manner led to numerous blocks in PHP, regardless of how it was induced. Postsynaptic knockdown
492 of *sra* disrupted acute, PhTx-induced PHP (**Figure 3**) while postsynaptic overexpression blocked
493 expression PHP induced by *GluRIIA* loss (**Figure 4**). Postsynaptic overexpression of *sra* did not
494 alter NMJ development (**Figure 5**), but it did uncover an increased amount of pCaMKII apposing
495 type-Ib boutons in a *GluRIIA* mutant background (**Figure 6**). For the neuron, we saw that
496 presynaptic knockdown of *sra* blocked chronic PHP **(Figure 7**) and presynaptic overexpression
497 also impaired it (**Figure 8**). Additionally, we were able to alleviate observed PHP blocks via

498 FK506, which is a calcineurin inhibitor (**Figures 9, 10**). We also showed that the maintenance of
499 PHP can be further potentiated via FK506, especially when the system is crippled by low
500 extracellular calcium (**Figure 11**). Finally, we demonstrated that concurrent neuronal and muscle
501 knockdown of the calcineurin subunit *CaNB* led to a weak block in acute PHP, but knockdown
502 specifically in the muscle strongly blocked the maintenance of PHP (**Figure 12**).

503 One possible model consistent with all the above is that the relative balance of calcineurin
504 function at NMJ tissues may control homeostatic signaling capacity. We believe that impairing
505 *sra* either pre- or postsynaptically (separately) leads to a PHP block as it can impair the relative
506 amounts of calcineurin activity between the two sides of the synapse. This idea may explain why
507 a combined pre- and postsynaptic *sra* impairment may not block PHP – even though calcineurin
508 activity is changed, the changes are reciprocal between both neuron and muscle.

509 This type of idea (relative pre- or postsynaptic balance) is new to the field of homeostatic
510 plasticity. But it is reminiscent of prior ideas that have emerged from studies of Hebbian plasticity.
511 One example is the Bienenstock-Cooper-Munro (BCM) rule for visual cortex learning. The BCM
512 rule dictates that either potentiation or depression can occur, but the direction of plasticity
513 ultimately depends upon the level of postsynaptic activity after a presynaptic neuron fires
514 (Bienenstock et al., 1982). By contrast, if activity is globally impaired (e.g., by blocking glutamate
515 receptors), no directional plasticity is possible (Bienenstock et al., 1982). In our case, we have an
516 opposite kind of phenomenon. Block of glutamate receptors initiates a form of homeostatic
517 plasticity. The expression of that plasticity can be blocked by tissue-specific manipulations to
518 calcineurin – but not global manipulations.

519

520 **Models of compensation: pharmacology vs. genetics, spatial vs. temporal**

521 The field of homeostatic synaptic plasticity faces a conundrum related to how PHP is
522 executed. Distinct acute pharmacological (PhTx) and chronic genetic manipulations (*GluRIIA*
523 loss) result in similar PHP expression mechanisms (Goel et al., 2017, Böhme et al., 2019, Müller et
524 al., 2012). Yet – depending upon the type of challenge used – important differences in PHP
525 expression have been observed. This has given rise to different models. Some groups have
526 proposed there exist differences in how the synapse executes PHP at phasic vs. tonic motor

527 terminals (Aponte-Santiago and Littleton, 2020, Genç and Davis, 2019, Newman et al., 2017, Sauvola et
528 al., 2021), depending upon pharamacological vs. genetic challenge. Recent characterization of
529 motor neuron-specific tools allow a refinement of analyses, at least in the context of presynaptic
530 terminals (Han et al., 2022, Aponte-Santiago et al., 2020, Wang et al., 2021). For a second model, a
531 recent study suggests that the type of pharmacological perturbation to glutamate receptors might
532 control the eventual response (Nair et al., 2021). A third model is that short-term and long-term
533 events that stabilize the NMJ are governed by genetically separable signaling systems (Brusich et
534 al., 2015, James et al., 2019, Spring et al., 2016, Yeates et al., 2017). This latter idea is analogous to
535 "early phase" and "late phase" events that trigger and consolidate Hebbian types of plasticity like
536 LTP (Bosch et al., 2014), and it gives rise to terms like "acute PHP" and "chronic PHP," similar to
537 what we have used here.

538 Importantly, these models are not mutually exclusive. Our data regarding calcineurin
539 regulation via Sarah is consistent with any of them. Intriguingly, misexpression of Sarah in the
540 postsynaptic muscle causes an increase in the levels of pCaMKII at boutons. By contrast,
541 downregulation of pCaMKII has been shown by other groups to be a sentinel of successful PHP
542 expression apposing type-Ib boutons, specifically when genetically impairing glutamate receptors
543 (Li et al., 2018, Newman et al., 2017). Whether or not such a mechanistic difference is dictated strictly
544 spatially or also temporally is yet to be full tested.

545

546 **Potential neuronal mechanisms for *sra* regulation of calcineurin to impact PHP**

547 Calcineurin regulation is the most notable function of *sra*. Decreased expression of *sra* increases
548 calcineurin activity, while increased *sra* via overexpression is presumed to decrease it (Chang et
549 al., 2003, Shaw and Chang, 2013). Our work suggests that an optimal amount of *sra* expression
550 underlies multiple different functions, each of which is necessary for robust homeostatic signaling.

551 Calcineurin has several presynaptic roles in various models that have been shown including
552 affecting synaptic vesicle exocytosis and endocytosis, axon remodeling and regulating
553 neurotransmitter release (Tarasova et al., 2018). One target of presynaptic calcineurin is to
554 dephosphorylate Synapsin 1 which can affect the mobilization of synaptic vesicles from the reserve
555 pool to active zones (Cesca et al., 2010, Jovanovic et al., 2001, Chi et al., 2003). For those studies,

556 opposing interactions between calcineurin and various kinases regulate vesicle mobilization. This
557 may explain why neuronal *sra* overexpression impaired acute PHP because increased *sra*
558 decreases calcineurin activity which may impair the mobilization of vesicles to active zones.
559 Challenges to NMJ function (e.g., *GluRIIA*^{SP16} or PhTx) consistently increase the number of
560 vesicles that are released, and failure to mobilize enough vesicles in response to a challenge may
561 lead to a failure for compensatory NLS quantal content increase and impair evoked release.

562 There are conflicting results on how the use of calcineurin inhibitors affects exocytosis.
563 They have been shown to increase the rate of exocytosis, show no change at all, or suppress
564 exocytosis (Yakel, 1997, Sim et al., 2003, Kumashiro et al., 2005). Specifically in the *Drosophila* NMJ,
565 calcineurin inhibition via FK506 has been shown to increase the endocytosis of synaptic vesicles,
566 while having no effect on the frequency of spontaneous events or the mean amplitude of evoked
567 events (Kuromi et al., 1997). This is contrary to the results of the current study where we showed
568 that mEPSP frequency is increased following FK506 incubation (**Figure 11D**). This difference
569 may be explained by the differences in concentration of FK506 that was used as previously, only
570 5µM and 10µM were tested. We see no change in mEPSP frequency at 10µM FK506, like previous
571 work as we only see the increase in spontaneous event frequency following 50µM FK506.
572 Alternatively, it is formally possible that FK506 could have some off-target effects at the NMJ that
573 affect parameters like mini frequency. Some possible ER-localized off-targets that could do this
574 are the ryanodine receptors (Ahern et al., 1994, Bultynck et al., 2000).

575 Calcineurin is believed to be a calcium-dependent regulator of endocytosis at both neuronal
576 and non-neuronal secretory cells (Wu et al., 2014). Calcineurin inhibitors slow endocytosis in
577 response to a small calcium influx but does not alter the speed of endocytosis in response to a large
578 calcium influx. If calcineurin is inhibiting synaptic vesicle recycling, this may explain why we see
579 a defect in chronic PHP following neuronal *sra* knockdown. Knockdown of *sra* leads to increased
580 calcineurin activity, and therefore increase inhibition of vesicular recycling. While this may not
581 lead to abnormal neurotransmission in the absence of a challenge, evoked amplitude may not be
582 maintained when chronically challenged due to an increased need for vesicle recycling in response
583 to the challenge.

584 Calcineurin may be affecting calcium influx as the targets of calcineurin in mouse NMJ
585 are L-type calcium channels (Gaydukov et al., 2013). Specifically, it was shown that calcineurin

586 downregulates neurotransmitter release by suppressing L-type calcium channels and calcium
587 release from intracellular stores through ryanodine receptors. In the *Drosophila* NMJ, it has
588 recently been shown that while L-type calcium channels are localized around active zones and
589 contribute to AP-triggered calcium influx, they are dispensable for evoked release (Krick et al.,
590 2021). However, it has not been shown if these channels are necessary for homeostatic signaling
591 processes. Calcium influx increases in response to both acute and chronic challenges to the synapse
592 (Müller and Davis, 2012). L-type calcium channels may be necessary for homeostatic compensation
593 as they not only serve as an additional entry point of calcium into the presynaptic compartment to
594 contribute to neurotransmitter release, but calcium entry through these channels also induces
595 calcium release from intracellular stores. In the current study, presynaptic loss of *sra* could lead to
596 increased calcineurin which may lead to increased inhibition of L-type calcium channels and not
597 allow for a large enough compensatory increase in calcium influx necessary to respond to a
598 homeostatic challenge.

599

600 **Possible postsynaptic mechanisms of *sra* to affect PHP through calcineurin regulation**

601 We showed that postsynaptic *sra* knockdown impaired acute homeostatic signaling (**Figure 3**)
602 while postsynaptic *sra* overexpression strongly blocked chronic homeostatic signaling (**Figure 4**).
603 It is well known that postsynaptically, calcineurin activation can lead to the dephosphorylation of
604 AMPA receptors that can lead to the internalization of them (D'Amelio et al., 2011, He et al., 2009,
605 Lin et al., 2000). Ionotropic glutamate receptor subunits that are localized to muscle in *Drosophila*
606 are *DGluRIIA* and *DGluRIIB*, both of which are AMPA/kainite type receptors (Betz et al., 1993,
607 Petersen et al., 1997). This presents a potential mechanism for how *sra* knockdown in the muscle
608 blocks PHP- decreased *sra* expression increases calcineurin activity which may lead to increased
609 internalization of postsynaptic glutamate receptors. A decrease in the amount of available
610 glutamate receptors may be detrimental when glutamate receptors are already being challenged
611 via philanthotoxin. However, we showed that the amount of GluRIII is increased in animals with
612 postsynaptic overexpression of *sra* (**Figure 6**). Our data suggest that *sra* overexpression
613 postsynaptically triggers a system to compensate for increased pCaMKII levels by trafficking in
614 more glutamate receptors to Ib boutons.

615 Our study also showed an increase in pCaMKII at Ib postsynaptic densities following
616 overexpression of *sra* postsynaptically in the chronically challenged *GluRIIA*^{SP16} null background
617 (**Figure 6**). Calcineurin is known to dephosphorylate I-1 which activates PPI to in turn
618 dephosphorylate and inactivate CaMKII (Tarasova et al., 2018). In the *Drosophila* NMJ, pCaMKII
619 levels have been found to be decreased following genetic glutamate receptor impairment (Newman
620 et al., 2017, Li et al., 2018, Goel et al., 2017). Additionally, postsynaptic overexpression of the
621 constitutively active phosphor-mimetic form of CaMKII^{T287D} blocks chronic PHP expression (Li et
622 al., 2018). Chronic overexpression of *sra* in the muscle decreases calcineurin function, which may
623 be leading to an increased amount of pCaMKII, contrary to what normally occurs in response to a
624 homeostatic challenge. While our data provides further evidence that the reduction of pCaMKII is
625 a necessary signal for functional PHP, it is unclear how decreased pCaMKII contributes to PHP.
626 It has been shown that mutations that alter CaMKII can impair the elaboration of the postsynaptic
627 subsynaptic reticulum and in turn result in defective PHP (SSR) (Koles et al., 2015, Koh et al., 1999).
628 It will be interesting to test how sra may interact with the development of the SSR and more
629 broadly how decreases in pCaMKII contribute to PHP.

630 It seems likely that Sarah's impact on PHP is at least partially through its role in calcineurin
631 regulation. Our data show that postsynaptic knockdown of the calcineurin subunit *CaNB* blocks
632 specifically the chronic but not acute PHP phase (**Figure 12**). These data support our experiment
633 on *sra* postsynaptic overexpression as both *sra* overexpression and *CaNB RNAi* decrease
634 calcineurin activity. This further strengthens the idea that postsynaptic decreases in calcineurin
635 activity through either manipulation blocks chronic PHP. It will be interesting to test if knockdown
636 of *CaNB* postsynaptically results in a similar increase in pCaMKII when chronically challenged
637 as was seen with *sra* postsynaptic overexpression (**Figure 6**). Calcineurin and CaMKII have been
638 shown to act as a switch-like mechanism both for controlling the direction of calcium dependent
639 growth cone tuning and for the regulation of cofilin activity and subsequently actin cytoskeletal
640 reorganization (Wen et al., 2004, Zhao et al., 2012). It is possible that at the *Drosophila* NMJ,
641 calcineurin and CaMKII act as a switch for regulating postsynaptic signaling that is necessary for
642 PHP maintenance.

643

644 **How *sra* could affect PHP through non-calcineurin regulating roles**

645 Previous work in rat cortex suggests that RCAN1 expression is upregulated following incubation
646 with Aβ (Lloret et al., 2011). The authors proposed that RCAN1 proteins not only inhibits
647 calcineurin but can also shift tau to a hyperphosphorylated state via inducing expression of GSK3β.
648 This provides evidence that RCAN1 proteins are linked to Alzheimer's and neurodegeneration.
649 Like this work and human studies, Aβ42-expressing *Drosophila* show increased Sra levels in the
650 brain (Lee et al., 2016). Genetic overexpression of *sra* in combination with Aβ42 impaired
651 locomotor activity and lifespan compared to overexpression of *sra* alone. However, data from
652 *Drosophila* suggest that upregulation of *sra* can be neuroprotective in the presence of amyloid
653 precursor protein (APP) by facilitating the transport of synaptic proteins and mitochondria (Shaw
654 and Chang, 2013). These conflicting results regarding the overexpression of *sra* demonstrate that
655 *sra* is involved with both APP and Aβ42 separate from its function of regulating calcineurin. It is
656 unclear if *sra* is working through calcineurin, APP, Aβ42 or other molecules to contribute to both
657 pre- and postsynaptic homeostatic signaling processes. This line of research may also lead to
658 examining other open questions such as how defective homeostatic synaptic processes may
659 contribute to neurodegeneration and other neural pathologies. It is known that most genes that are
660 necessary for PHP are linked to neural disorders and pathologies such as autism spectrum
661 disorders, schizophrenia, Fragile X Syndrome, migraine, and epilepsy (Wondolowski and Dickman,
662 2013, Frank et al., 2020).

663 Another idea for how the expression of *sra* may be regulating PHP is through its effects on
664 mitochondrial function. Both increases and decreases in *sra* have been shown to result in decreased
665 ATP levels, increased ROS production, decreased mitochondrial DNA in *Drosophila* heads,
666 decreased mitochondrial size, and increased mitochondrial number (Chang and Min, 2005). This is
667 independent from its function of regulating calcineurin as decreasing calcineurin activity in *sra*
668 mutants did not rescue mitochondrial enzymatic activity. Recent work also indicates that
669 Mitochondrial Complex I (MCI) is necessary for synapse function and plasticity at the *Drosophila*
670 NMJ (Mallik and Frank, 2022). Genetic knockdown or pharmacological inhibition of MCI impaired
671 neurotransmission, reduced NMJ growth and altered NMJ morphology.

672

673 **Acute versus chronic PHP expression with single tissue contributions**

674 There is strong evidence to suggest that there are shared mechanisms underlying both the acute
675 and chronic forms of PHP signaling as both forms display robust increases in readily releasable
676 pool (RRP) size and Ca_V2-mediated calcium influx that result in increases in quantal content
677 necessary for function PHP (Davis and Müller, 2015, Müller and Davis, 2012). Recent work has found
678 that the acute and chronic forms of PHP are functionally separable (James et al., 2019). Our data
679 support this idea by showing minimal overlap in a specific *sra* impairment in a specific tissue. For
680 example, *sra* knockdown postsynaptically only blocked acute PHP while leaving the chronic phase
681 intact; conversely, *sra* overexpression postsynaptically did not impair acute PHP while blocking
682 chronic PHP. These data demonstrate that *sra* is tightly regulated as both too much and too little
683 *sra* can disrupt PHP.

684 Our *CaNB* knockdown data also support the separation of the acute and chronic phases of
685 PHP as global knockdown led to a weak impairment in acute PHP while leaving chronic PHP
686 intact. Conversely, postsynaptic-specific knockdown led to a strong block in chronic PHP but left
687 acute PHP intact. These data support the separation of acute and chronic PHP as *sra* and *CaNB*
688 expression are likely regulating different processes at different timepoints that integrate to produce
689 functional PHP.

690 Other work has suggested that PHP pathways converge onto the same targets (Goel et al.,
691 2017). While it is possible that discrete signaling pathways converge, it is more likely that there is
692 some degree of convergence while also some amount of separate signaling systems. It will be
693 important for future studies to test how the individual influences of molecules from distinct
694 synaptic tissues underly the different phases of PHP to promote a fully functional PHP signaling
695 system. Collectively, our data indicate that some situations where PHP is blocked in the short run
696 are eventually resolved over developmental time if the synapse is given sufficient time to grow
697 and implement an array of compensatory mechanisms at its disposal (Goel et al., 2019). Conversely
698 there could be other situations where the synapse has a capacity for a quick response but fails to
699 respond after long periods of continuous challenge.

700

701

702 **References**

AHERN, G. P., JUNANKAR, P. R. & DULHUNTY, A. F. 1994. Single channel activity of the ryanodine receptor calcium release channel is modulated by FK-506. *FEBS Lett,* 352**,** 369-74.

ANDRE, E. A., FORCELLI, P. A. & PAK, D. T. 2018. What goes up must come down: homeostatic synaptic plasticity strategies in neurological disease. *Future Neurol,* 13**,** 13-21.

APONTE-SANTIAGO, N. A. & LITTLETON, J. T. 2020. Synaptic Properties and Plasticity Mechanisms of Invertebrate Tonic and Phasic Neurons. *Front Physiol,* 11**,** 611982.

APONTE-SANTIAGO, N. A., ORMEROD, K. G., AKBERGENOVA, Y. & LITTLETON, J. T. 2020. Synaptic Plasticity Induced by Differential Manipulation of Tonic and Phasic Motoneurons in Drosophila. *J Neurosci,* 40**,** 6270-6288.

BAUMGÄRTEL, K. & MANSUY, I. M. 2012. Neural functions of calcineurin in synaptic plasticity and memory. *Learn Mem,* 19**,** 375-84.

BETZ, H., SCHUSTER, C., ULTSCH, A. & SCHMITT, B. 1993. Molecular biology of ionotropic glutamate receptors in Drosophila melanogaster. *Trends in Pharmacological Sciences,* 14**,** 428-431.

BIENENSTOCK, E. L., COOPER, L. N. & MUNRO, P. W. 1982. Theory for the development of neuron selectivity: orientation specificity and binocular interaction in visual cortex. *J Neurosci,* 2**,** 32-48.

BLISS, T. V. P., COLLINGRIDGE, G. L. & MORRIS, R. G. M. 2014. Synaptic plasticity in health and disease: introduction and overview. *Philosophical Transactions of the Royal Society B: Biological Sciences,* 369**,** 20130129.

BÖHME, M. A., MCCARTHY, A. W., GRASSKAMP, A. T., BEUSCHEL, C. B., GOEL, P., JUSYTE, M., LABER, D., HUANG, S., REY, U., PETZOLDT, A. G., LEHMANN, M., GOTTFERT, F., HAGHIGHI, P., HELL, S. W., OWALD, D., DICKMAN, D., SIGRIST, S. J. & WALTER, A. M. 2019. Rapid active zone remodeling consolidates presynaptic potentiation. *Nat Commun,* 10**,** 1085.

BOSCH, M., CASTRO, J., SANEYOSHI, T., MATSUNO, H., SUR, M. & HAYASHI, Y. 2014. Structural and molecular remodeling of dendritic spine substructures during long-term potentiation. *Neuron,* 82**,** 444-59.

BRUSICH, D. J., SPRING, A. M. & FRANK, C. A. 2015. A single-cross, RNA interference-based genetic tool for examining the long-term maintenance of homeostatic plasticity. *Front Cell Neurosci,* 9**,** 107.

BUDNIK, V., KOH, Y. H., GUAN, B., HARTMANN, B., HOUGH, C., WOODS, D. & GORCZYCA, M. 1996. Regulation of synapse structure and function by the Drosophila tumor suppressor gene dlg. *Neuron,* 17**,** 627-40.

BULTYNCK, G., DE SMET, P., WEIDEMA, A. F., VER HEYEN, M., MAES, K., CALLEWAERT, G., MISSIAEN, L., PARYS, J. B. & DE SMEDT, H. 2000. Effects of the immunosuppressant FK506 on intracellular Ca2+ release and Ca2+ accumulation mechanisms. *J Physiol,* 525 Pt 3**,** 681-93.

CESCA, F., BALDELLI, P., VALTORTA, F. & BENFENATI, F. 2010. The synapsins: key actors of synapse function and plasticity. *Prog Neurobiol,* 91**,** 313-48.

CHANG, K. T. & MIN, K. T. 2005. Drosophila melanogaster homolog of Down syndrome critical region 1 is critical for mitochondrial function. *Nat Neurosci,* 8**,** 1577-85.

CHANG, K. T., SHI, Y.-J. & MIN, K.-T. 2003. The Drosophila homolog of Down's syndrome critical region 1 gene regulates learning: Implications for mental retardation. *Proceedings of the National Academy of Sciences,* 100**,** 15794-15799.

CHI, P., GREENGARD, P. & RYAN, T. A. 2003. Synaptic vesicle mobilization is regulated by distinct synapsin I phosphorylation pathways at different frequencies. *Neuron,* 38**,** 69-78.

CLARDY, J. 1995. The chemistry of signal transduction. *Proceedings of the National Academy of Sciences of the United States of America,* 92**,** 56-61.

D'AMELIO, M., CAVALLUCCI, V., MIDDEI, S., MARCHETTI, C., PACIONI, S., FERRI, A., DIAMANTINI, A., DE ZIO, D., CARRARA, P., BATTISTINI, L., MORENO, S., BACCI, A., AMMASSARI-TEULE, M., MARIE, H. & CECCONI, F. 2011. Caspase-3 triggers early synaptic dysfunction in a mouse model of Alzheimer's disease. *Nat Neurosci,* 14**,** 69-76.

DAVIS, G. W. 2006. Homeostatic control of neural activity: from phenomenology to molecular design. *Annu Rev Neurosci,* 29**,** 307-23.

DAVIS, G. W., DIANTONIO, A., PETERSEN, S. A. & GOODMAN, C. S. 1998. Postsynaptic PKA controls quantal size and reveals a retrograde signal that regulates presynaptic transmitter release in Drosophila. *Neuron,* 20**,** 305-15.

DAVIS, G. W. & MÜLLER, M. 2015. Homeostatic control of presynaptic neurotransmitter release. *Annu Rev Physiol,* 77**,** 251-70.

DEL CASTILLO, J. & KATZ, B. 1954. Quantal components of the end-plate potential. *J Physiol,* 124**,** 560-73.

DIANTONIO, A., PETERSEN, S. A., HECKMANN, M. & GOODMAN, C. S. 1999. Glutamate receptor expression regulates quantal size and quantal content at the Drosophila neuromuscular junction. *J Neurosci,* 19**,** 3023-32.

772 DICKMAN, D. & WONDOLOWSKI, J. 2013. Emerging links between homeostatic synaptic
773 plasticity and neurological disease. *Frontiers in Cellular Neuroscience,* 7.

774 FRANK, C. A. 2014a. Homeostatic plasticity at the Drosophila neuromuscular junction.
775 *Neuropharmacology,* 78**,** 63-74.

776 FRANK, C. A. 2014b. How voltage-gated calcium channels gate forms of homeostatic synaptic
777 plasticity. *Front Cell Neurosci,* 8**,** 40.

778 FRANK, C. A., JAMES, T. D. & MÜLLER, M. 2020. Homeostatic control of Drosophila
779 neuromuscular junction function. *Synapse,* 74**,** e22133.

780 FRANK, C. A., KENNEDY, M. J., GOOLD, C. P., MAREK, K. W. & DAVIS, G. W. 2006.
781 Mechanisms underlying the rapid induction and sustained expression of synaptic
782 homeostasis. *Neuron,* 52**,** 663-77.

783 FRANK, C. A., PIELAGE, J. & DAVIS, G. W. 2009. A presynaptic homeostatic signaling system
784 composed of the Eph receptor, ephexin, Cdc42, and CaV2.1 calcium channels. *Neuron,* 61**,**
785 556-69.

786 FURMAN, J. L. & NORRIS, C. M. 2014. Calcineurin and glial signaling: neuroinflammation and
787 beyond. *J Neuroinflammation,* 11**,** 158.

788 GAYDUKOV, A., TARASOVA, E. & BALEZINA, O. 2013. Calcium-dependent phosphatase
789 calcineurin downregulates evoked neurotransmitter release in neuromuscular junctions of
790 mice. *Neurochemical Journal,* 7**,** 29-33.

791 GENÇ, O. & DAVIS, G. W. 2019. Target-wide Induction and Synapse Type-Specific Robustness
792 of Presynaptic Homeostasis. *Curr Biol,* 29**,** 3863-3873 e2.

793 GOEL, P. & DICKMAN, D. 2018. Distinct homeostatic modulations stabilize reduced
794 postsynaptic receptivity in response to presynaptic DLK signaling. *Nat Commun,* 9**,** 1856.

795 GOEL, P., KHAN, M., HOWARD, S., KIM, G., KIRAGASI, B., KIKUMA, K. & DICKMAN,
796 D. 2019. A screen for synaptic growth mutants reveals mechanisms that stabilize synaptic
797 strength. *J Neurosci*.

798 GOEL, P., LI, X. & DICKMAN, D. 2017. Disparate Postsynaptic Induction Mechanisms
799 Ultimately Converge to Drive the Retrograde Enhancement of Presynaptic Efficacy. *Cell*
800 *Rep,* 21**,** 2339-2347.

801 GREENSPAN, R. J. 2004. *Fly pushing : the theory and practice of Drosophila genetics,* Cold
802 Spring Harbor, N.Y., Cold Spring Harbor Laboratory Press.

803 HAN, Y., CHIEN, C., GOEL, P., HE, K., PINALES, C., BUSER, C. & DICKMAN, D. 2022.
804 Botulinum neurotoxin accurately separates tonic vs. phasic transmission and reveals
805 heterosynaptic plasticity rules in Drosophila. *Elife,* 11.

806 HARRIS, C. D., ERMAK, G. & DAVIES, K. J. 2005. Multiple roles of the DSCR1 (Adapt78 or
807 RCAN1) gene and its protein product calcipressin 1 (or RCAN1) in disease. *Cell Mol Life*
808 *Sci,* 62**,** 2477-86.

809 HARRIS, N., BRAISER, D. J., DICKMAN, D. K., FETTER, R. D., TONG, A. & DAVIS, G. W.
810 2015. The Innate Immune Receptor PGRP-LC Controls Presynaptic Homeostatic
811 Plasticity. *Neuron,* 88**,** 1157-64.

812 HAZELRIGG, T., LEVIS, R. & RUBIN, G. M. 1984. Transformation of white locus DNA in
813 drosophila: dosage compensation, zeste interaction, and position effects. *Cell,* 36**,** 469-81.

814 HE, K., SONG, L., CUMMINGS, L. W., GOLDMAN, J., HUGANIR, R. L. & LEE, H.-K. 2009.
815 Stabilization of Ca²⁺-permeable AMPA receptors at perisynaptic sites by
816 GluR1-S845 phosphorylation. *Proceedings of the National Academy of Sciences,* 106**,**
817 20033-20038.

818 HORNER, V. L., CZANK, A., JANG, J. K., SINGH, N., WILLIAMS, B. C., PURO, J., KUBLI,
819 E., HANES, S. D., MCKIM, K. S., WOLFNER, M. F. & GOLDBERG, M. L. 2006. The
820 Drosophila Calcipressin Sarah Is Required for Several Aspects of Egg Activation. *Current*
821 *Biology,* 16**,** 1441-1446.

822 JAMES, T. D., ZWIEFELHOFER, D. J. & FRANK, C. A. 2019. Maintenance of homeostatic
823 plasticity at the Drosophila neuromuscular synapse requires continuous IP3-directed
824 signaling. *eLife,* 8.

825 JAN, L. Y. & JAN, Y. N. 1976. Properties of the larval neuromuscular junction in Drosophila
826 melanogaster. *J Physiol,* 262**,** 189-214.

827 JOVANOVIC, J. N., SIHRA, T. S., NAIRN, A. C., HEMMINGS, H. C., JR., GREENGARD, P.
828 & CZERNIK, A. J. 2001. Opposing changes in phosphorylation of specific sites in
829 synapsin I during Ca2+-dependent glutamate release in isolated nerve terminals. *J*
830 *Neurosci,* 21**,** 7944-53.

831 KADAMUR, G. & ROSS, E. M. 2013. Mammalian phospholipase C. *Annu Rev Physiol,* 75**,** 127-
832 54.

833 KIKUMA, K., LI, X., PERRY, S., LI, Q., GOEL, P., CHEN, C., KIM, D., STAVROPOULOS, N.
834 & DICKMAN, D. 2019. Cul3 and insomniac are required for rapid ubiquitination of
835 postsynaptic targets and retrograde homeostatic signaling. *Nat Commun,* 10**,** 2998.

836 KINGSBURY, T. J. & CUNNINGHAM, K. W. 2000. A conserved family of calcineurin
837 regulators. *Genes & development,* 14**,** 1595-1604.

838 KOH, Y. H., POPOVA, E., THOMAS, U., GRIFFITH, L. C. & BUDNIK, V. 1999. Regulation of
839 DLG Localization at Synapses by CaMKII-Dependent Phosphorylation. *Cell,* 98**,** 353-363.

840 KOLES, K., MESSELAAR, E. M., FEIGER, Z., YU, C. J., FRANK, C. A. & RODAL, A. A.
841 2015. The EHD protein Past1 controls postsynaptic membrane elaboration and synaptic
842 function. *Molecular Biology of the Cell,* 26**,** 3275-3288.

843 KRICK, N., RYGLEWSKI, S., PICHLER, A., BIKBAEV, A., GÖTZ, T., KOBLER, O., HEINE,
844 M., THOMAS, U. & DUCH, C. 2021. Separation of presynaptic Ca_v2 and Ca_v1 channel
845 function in synaptic vesicle exo- and endocytosis by the membrane anchored Ca^{2+} pump
846 PMCA. *Proceedings of the National Academy of Sciences,* 118**,** e2106621118.

847 KUMASHIRO, S., LU, Y. F., TOMIZAWA, K., MATSUSHITA, M., WEI, F. Y. & MATSUI, H.
848 2005. Regulation of synaptic vesicle recycling by calcineurin in different vesicle pools.
849 *Neurosci Res,* 51**,** 435-43.

850 KUROMI, H., YOSHIHARA, M. & KIDOKORO, Y. 1997. An inhibitory role of calcineurin in
851 endocytosis of synaptic vesicles at nerve terminals of Drosophila larvae. *Neurosci Res,* 27**,**
852 101-13.

853 LEE, J. I., DHAKAL, B. K., LEE, J., BANDYOPADHYAY, J., JEONG, S. Y., EOM, S. H., KIM,
854 D. H. & AHNN, J. 2003. The Caenorhabditis elegans Homologue of Down Syndrome
855 Critical Region 1, RCN-1, Inhibits Multiple Functions of the Phosphatase Calcineurin.
856 *Journal of Molecular Biology,* 328**,** 147-156.

857 LEE, S., BANG, S. M., HONG, Y. K., LEE, J. H., JEONG, H., PARK, S. H., LIU, Q. F., LEE, I.
858 S. & CHO, K. S. 2016. The calcineurin inhibitor Sarah (Nebula) exacerbates Abeta42
859 phenotypes in a Drosophila model of Alzheimer's disease. *Dis Model Mech,* 9**,** 295-306.

860 LI, X., GOEL, P., CHEN, C., ANGAJALA, V., CHEN, X. & DICKMAN, D. K. 2018. Synapse-
861 specific and compartmentalized expression of presynaptic homeostatic potentiation. *Elife,*
862 7.

863 LIN, D. M. & GOODMAN, C. S. 1994. Ectopic and increased expression of Fasciclin II alters
864 motoneuron growth cone guidance. *Neuron,* 13**,** 507-23.

865 LIN, J. W., JU, W., FOSTER, K., LEE, S. H., AHMADIAN, G., WYSZYNSKI, M., WANG, Y.
866 T. & SHENG, M. 2000. Distinct molecular mechanisms and divergent endocytotic
867 pathways of AMPA receptor internalization. *Nat Neurosci,* 3**,** 1282-90.

868 LIU, J., FARMER, J. D., JR., LANE, W. S., FRIEDMAN, J., WEISSMAN, I. & SCHREIBER, S.
869 L. 1991. Calcineurin is a common target of cyclophilin-cyclosporin A and FKBP-FK506
870 complexes. *Cell,* 66**,** 807-15.

871 LLORET, A., BADIA, M. C., GIRALDO, E., ERMAK, G., ALONSO, M. D., PALLARDÓ, F.
872 V., DAVIES, K. J. & VIÑA, J. 2011. Amyloid-β toxicity and tau hyperphosphorylation
873 are linked via RCAN1 in Alzheimer's disease. *J Alzheimers Dis,* 27**,** 701-9.

874 MALLIK, B. & FRANK, C. A. 2022. Roles for Mitochondrial Complex I Subunits in Regulating
875 Synaptic Transmission and Growth. *Frontiers in Neuroscience,* 16.

MARDER, E. 2012. Neuromodulation of neuronal circuits: back to the future. *Neuron,* 76**,** 1-11.

MARRUS, S. B., PORTMAN, S. L., ALLEN, M. J., MOFFAT, K. G. & DIANTONIO, A. 2004. Differential Localization of Glutamate Receptor Subunits at the Drosophila Neuromuscular Junction. *The Journal of Neuroscience,* 24**,** 1406.

MCLACHLAN, E. M. & MARTIN, A. R. 1981. Non-linear summation of end-plate potentials in the frog and mouse. *J Physiol,* 311**,** 307-24.

MENON, K. P., CARRILLO, R. A. & ZINN, K. 2013. Development and plasticity of the Drosophila larval neuromuscular junction. *Wiley Interdiscip Rev Dev Biol,* 2**,** 647-70.

MÜLLER, M. & DAVIS, G. W. 2012. Transsynaptic control of presynaptic Ca^{2+} influx achieves homeostatic potentiation of neurotransmitter release. *Current biology : CB,* 22**,** 1102-1108.

MÜLLER, M., GENÇ, Ö. & DAVIS, G. W. 2015. RIM-Binding Protein Links Synaptic Homeostasis to the Stabilization and Replenishment of High Release Probability Vesicles. *Neuron*.

MÜLLER, M., LIU, K. S., SIGRIST, S. J. & DAVIS, G. W. 2012. RIM Controls Homeostatic Plasticity through Modulation of the Readily-Releasable Vesicle Pool. *J Neurosci,* 32**,** 16574-85.

MUSSON, R. E. & SMIT, N. P. 2011. Regulatory mechanisms of calcineurin phosphatase activity. *Curr Med Chem,* 18**,** 301-15.

NAIR, A. G., MUTTATHUKUNNEL, P. & MÜLLER, M. 2021. Distinct molecular pathways govern presynaptic homeostatic plasticity. *Cell Rep,* 37**,** 110105.

NAKAI, Y., HORIUCHI, J., TSUDA, M., TAKEO, S., AKAHORI, S., MATSUO, T., KUME, K. & AIGAKI, T. 2011. Calcineurin and its regulator sra/DSCR1 are essential for sleep in Drosophila. *J Neurosci,* 31**,** 12759-66.

NEWMAN, Z. L., HOAGLAND, A., AGHI, K., WORDEN, K., LEVY, S. L., SON, J. H., LEE, L. P. & ISACOFF, E. Y. 2017. Input-Specific Plasticity and Homeostasis at the Drosophila Larval Neuromuscular Junction. *Neuron,* 93**,** 1388-1404 e10.

PARK, J., OH, Y. & CHUNG, K. C. 2009. Two key genes closely implicated with the neuropathological characteristics in Down syndrome: DYRK1A and RCAN1. *BMB Rep,* 42**,** 6-15.

PETERSEN, S. A., FETTER, R. D., NOORDERMEER, J. N., GOODMAN, C. S. & DIANTONIO, A. 1997. Genetic analysis of glutamate receptors in Drosophila reveals a retrograde signal regulating presynaptic transmitter release. *Neuron,* 19**,** 1237-48.

PHILIP, F., KADAMUR, G., SILOS, R. G., WOODSON, J. & ROSS, E. M. 2010. Synergistic activation of phospholipase C-beta3 by Galpha(q) and Gbetagamma describes a simple two-state coincidence detector. *Curr Biol,* 20**,** 1327-35.

POZO, K. & GODA, Y. 2010. Unraveling mechanisms of homeostatic synaptic plasticity. *Neuron,* 66**,** 337-51.

RUSNAK, F. & MERTZ, P. 2000. Calcineurin: form and function. *Physiol Rev,* 80**,** 1483-521.

SAUVOLA, C. W., AKBERGENOVA, Y., CUNNINGHAM, K. L., APONTE-SANTIAGO, N. A. & LITTLETON, J. T. 2021. The decoy SNARE Tomosyn sets tonic versus phasic release properties and is required for homeostatic synaptic plasticity. *Elife,* 10.

SHAW, J. L. & CHANG, K. T. 2013. Nebula/DSCR1 Upregulation Delays Neurodegeneration and Protects against APP-Induced Axonal Transport Defects by Restoring Calcineurin and GSK-3β Signaling. *PLOS Genetics,* 9**,** e1003792.

SIGAL, N. H. & DUMONT, F. J. 1992. Cyclosporin A, FK-506, and rapamycin: pharmacologic probes of lymphocyte signal transduction. *Annu Rev Immunol,* 10**,** 519-60.

SIM, A. T., BALDWIN, M. L., ROSTAS, J. A., HOLST, J. & LUDOWYKE, R. I. 2003. The role of serine/threonine protein phosphatases in exocytosis. *Biochem J,* 373**,** 641-59.

SPRING, A. M., BRUSICH, D. J. & FRANK, C. A. 2016. C-terminal Src Kinase Gates Homeostatic Synaptic Plasticity and Regulates Fasciclin II Expression at the Drosophila Neuromuscular Junction. *PLoS Genet,* 12**,** e1005886.

STEWART, B., ATWOOD, H., RENGER, J., WANG, J. & WU, C. 1994. Improved stability of Drosophila larval neuromuscular preparations in haemolymph-like physiological solutions A Neuroethology, sensory, neural, and behavioral physiology.

SWANSON, S. K., BORN, T., ZYDOWSKY, L. D., CHO, H., CHANG, H. Y., WALSH, C. T. & RUSNAK, F. 1992. Cyclosporin-mediated inhibition of bovine calcineurin by cyclophilins A and B. *Proc Natl Acad Sci U S A,* 89**,** 3741-5.

TAKEO, S., SWANSON, S. K., NANDANAN, K., NAKAI, Y., AIGAKI, T., WASHBURN, M. P., FLORENS, L. & HAWLEY, R. S. 2012. Shaggy/glycogen synthase kinase 3beta and phosphorylation of Sarah/regulator of calcineurin are essential for completion of Drosophila female meiosis. *Proc Natl Acad Sci U S A,* 109**,** 6382-9.

TAKEO, S., TSUDA, M., AKAHORI, S., MATSUO, T. & AIGAKI, T. 2006. The Calcineurin Regulator Sra Plays an Essential Role in Female Meiosis in Drosophila. *Current Biology,* 16**,** 1435-1440.

TARASOVA, E. O., GAYDUKOV, A. E. & BALEZINA, O. P. 2018. Calcineurin and Its Role in Synaptic Transmission. *Biochemistry (Mosc),* 83**,** 674-689.

TOMITA, J., MITSUYOSHI, M., UENO, T., ASO, Y., TANIMOTO, H., NAKAI, Y., AIGAKI, T., KUME, S. & KUME, K. 2011. Pan-Neuronal Knockdown of Calcineurin Reduces Sleep in the Fruit Fly, Drosophila melanogaster. *The Journal of Neuroscience,* 31**,** 13137-13146.

TONONI, G. & CIRELLI, C. 2006. Sleep function and synaptic homeostasis. *Sleep Medicine Reviews,* 10**,** 49-62.

VICTOR, R. G., THOMAS, G. D., MARBAN, E. & O'ROURKE, B. 1995. Presynaptic modulation of cortical synaptic activity by calcineurin. *Proceedings of the National Academy of Sciences of the United States of America,* 92**,** 6269-6273.

VONHOFF, F. & KESHISHIAN, H. 2017. In Vivo Calcium Signaling during Synaptic Refinement at the Drosophila Neuromuscular Junction. *The Journal of Neuroscience,* 37**,** 5511-5526.

WANG, T., HAUSWIRTH, A. G., TONG, A., DICKMAN, D. K. & DAVIS, G. W. 2014. Endostatin Is a Trans-Synaptic Signal for Homeostatic Synaptic Plasticity. *Neuron,* 83**,** 616-629.

WANG, Y., LOBB-RABE, M., ASHLEY, J., ANAND, V. & CARRILLO, R. A. 2021. Structural and Functional Synaptic Plasticity Induced by Convergent Synapse Loss in the Drosophila Neuromuscular Circuit. *J Neurosci,* 41**,** 1401-1417.

WEN, Z., GUIRLAND, C., MING, G. L. & ZHENG, J. Q. 2004. A CaMKII/calcineurin switch controls the direction of Ca(2+)-dependent growth cone guidance. *Neuron,* 43**,** 835-46.

WEYHERSMÜLLER, A., HALLERMANN, S., WAGNER, N. & EILERS, J. 2011. Rapid active zone remodeling during synaptic plasticity. *J Neurosci,* 31**,** 6041-52.

WONDOLOWSKI, J. & DICKMAN, D. 2013. Emerging links between homeostatic synaptic plasticity and neurological disease. *Front Cell Neurosci,* 7**,** 223.

WU, X.-S., ZHANG, Z., ZHAO, W.-D., WANG, D., LUO, F. & WU, L.-G. 2014. Calcineurin is universally involved in vesicle endocytosis at neuronal and nonneuronal secretory cells. *Cell reports,* 7**,** 982-988.

YAKEL, J. L. 1997. Calcineurin regulation of synaptic function: from ion channels to transmitter release and gene transcription. *Trends Pharmacol Sci,* 18**,** 124-34.

YEATES, C. J. & FRANK, C. A. 2021. Homeostatic Depression Shows Heightened Sensitivity to Synaptic Calcium. *Front Cell Neurosci,* 15**,** 618393.

YEATES, C. J., ZWIEFELHOFER, D. J. & FRANK, C. A. 2017. The Maintenance of Synaptic Homeostasis at the Drosophila Neuromuscular Junction Is Reversible and Sensitive to High Temperature. *eNeuro,* 4.

977 YOUNGER, M. A., MÜLLER, M., TONG, A., PYM, E. C. & DAVIS, G. W. 2013. A presynaptic
978 ENaC channel drives homeostatic plasticity. *Neuron,* 79**,** 1183-96.

979 ZHAO, J.-W., GAO, Z.-L., ZHANG, H.-Y., JI, Q.-Y., WANG, H., YANG, Y.-D., XING, F.-J.,
980 MENG, L.-J. & WANG, Y. 2012. Regulation of Cofilin Activity by CaMKII and
981 Calcineurin. *The American Journal of the Medical Sciences,* 344**,** 462-472.

982

983

984 **Figure 1.** Dual pre and postsynaptic knockdown or overexpression of *sra* does not block PHP **(A-**
985 **C)** Quantification showing average mEPSP amplitude, EPSP amplitude, and NLS quantal content
986 in pre + post-GAL4 control and pre + post-GAL4 driven *sra RNAi*. Black points show DMSO
987 control synapses, green points show synapses treated with PhTx, and magenta points show animals
988 chronically challenged with *GluRIII RNAi*. **(D, H)** Representative electrophysiological traces of
989 EPSPs (above) and mEPSPs (below). Scale bars for all traces are y = 10 mV (1mV), x = 20 ms
990 (500 ms) for EPSPs (mEPSPs). **(E-G)** Quantification showing average mEPSP amplitude, EPSP
991 amplitude, and NLS quantal content in pre + post-GAL4 control and pre + post-GAL4 driven *sra*
992 overexpression (OE). Black points show DMSO control synapses, green points show synapses
993 treated with PhTx, and magenta points show animals chronically challenged with *GluRIII RNAi*.
994 *p<0.05, **p<0.01, ***p<0.001 by Multiple Student's T-test and corrected for multiple
995 comparisons using the Holm-Sidak method. DMSO controls were compared to PhTx and *GluRIII*
996 *RNAi* synapses for driver controls and separately for *sra RNAi* or OE.

997

998 **Figure 2.** Global *sra* mutation does not preclude PHP but does show an evoked amplitude decrease
999 in low calcium conditions. **(A-C)** Quantification showing average mEPSP, EPSP amplitude, and
1000 NLS quantal content in $sra^{Mi06345}$, $sra^{Mi06345}/Df(3R)sbd^{104}$, and $GluRIIA^{SP16}$;
1001 $sra^{Mi06345}/Df(3R)sbd^{104}$. **(D, H)** Representative electrophysiological traces of EPSPs (above) and
1002 mEPSPs (below). Scale bars for all traces are y = 10 mV (1mV), x = 20 ms (500 ms) for EPSPs
1003 (mEPSPs). **(E-G)** Experiments conducted in low calcium (0.2mM). Quantification showing
1004 average mEPSP, EPSP amplitude, and NLS quantal content in $sra^{Mi06345}$, $sra^{Mi06345}/Df(3R)sbd^{104}$,
1005 and $GluRIIA^{SP16}$; $sra^{Mi06345}/Df(3R)sbd^{104}$. Ordinary one-way ANOVAs were used to compare each
1006 genotype followed by a Tukey's HSD test for multiple comparisons. *p<0.05, **p<0.01,
1007 ***p<0.001.

1008

1009 **Figure 3.** Acute expression of presynaptic homeostatic potentiation requires muscle expression of
1010 *sra*, but maintenance does not. **(A-C)** Quantification showing average mEPSP amplitude, EPSP
1011 amplitude, and NLS quantal content in post-GAL4 control and post-GAL4 driven *sra* RNAi. Black
1012 points show DMSO control synapses, while green points show synapses treated with PhTx. **(D, H)**
1013 Representative electrophysiological traces of EPSPs (above) and mEPSPs (below). Scale bars for

1014 all traces are y = 10 mV (1mV), x = 20 ms (500 ms) for EPSPs (mEPSPs). **(E-G)** Quantification
1015 showing average mEPSP amplitude, EPSP amplitude, and NLS quantal content in post-GAL4
1016 control and post-GAL4 driven *sra* RNAi in both the presence and absence of $GluRIIA^{SP16}$.
1017 *p<0.05, **p<0.01, ***p<0.001 by Student's T-test versus non-challenged genetic control.

1018

1019 **Figure 4.** Maintenance of presynaptic homeostatic potentiation is impaired by muscle
1020 overexpression of *sra*, but acute expression is not. **(A-C)** Quantification showing average mEPSP
1021 amplitude, EPSP amplitude, and NLS quantal content in post-GAL4 control and post-GAL4 driven
1022 *sra* overexpression (OE). Black points show DMSO control synapses, while green points show
1023 synapses treated with PhTx. **(D, H)** Representative electrophysiological traces of EPSPs (above)
1024 and mEPSPs (below). Scale bars for all traces are y = 10 mV (1mV), x = 20 ms (500 ms) for EPSPs
1025 (mEPSPs). **(E-G)** Quantification showing average mEPSP amplitude, EPSP amplitude, and NLS
1026 quantal content in post-GAL4 control and post-GAL4 driven *sra* OE in both the presence and
1027 absence of $GluRIIA^{SP16}$. *p<0.05, **p<0.01, ***p<0.001 by Student's T-test versus non-
1028 challenged genetic control.

1029

1030 **Figure 5.** Postsynaptic *sra* overexpression does not impair synapse development. **(A-F)** NMJs
1031 were co-stained with anti-DLG (magenta) and anti-Synapsin antibodies (green) to visualize
1032 synaptic boutons. **(G)** NMJ growth was assessed by bouton counting at abdominal segments A2
1033 and A3, muscle 6/7, based on postsynaptic DLG staining and checking for presynaptic Synapsin.
1034 **(H)** Bouton counts were normalized per unit of muscle 6/7 area. Ordinary one-way ANOVAs were
1035 used to compare each genotype within each segment followed by a Tukey's HSD test for multiple
1036 comparisons. *p<0.05, **p<0.01, ***p<0.001.

1037

1038 **Figure 6.** Postsynaptic *sra* overexpression disrupts pCaMKII in Ib postsynaptic densities. **(A)**
1039 Maximum-intensity projections of pCaMKII (magenta) and GluRIII (green). Merged images of
1040 both channels shown in top row. Representative bouton maximum-intensity projections of
1041 pCaMKII (middle row) and GluRIII (bottom row) are shown as heat maps. **(B)** Quantification of
1042 pCaMKII intensity as a percentage relative to wild type boutons. Each point represents the

1043 intensity at an individual Ib postsynaptic density. **(C)** Quantification of GluRIII intensity as a
1044 percentage relative to wild type boutons. Ordinary one-way ANOVAs were used to compare each
1045 genotype followed by a Tukey's HSD test for multiple comparisons. *p<0.05, **p<0.01,
1046 ***p<0.001.

1047

1048 **Figure 7.** Maintenance of presynaptic homeostatic potentiation is impaired by neuronal
1049 knockdown of *sra*, but acute expression is not. **(A-C)** Quantification showing average mEPSP
1050 amplitude, EPSP amplitude, and NLS quantal content in pre-GAL4 control and pre-GAL4 driven
1051 *sra* RNAi. Black points show DMSO control synapses, while green points show synapses treated
1052 with PhTx. **(D, H)** Representative electrophysiological traces of EPSPs (above) and mEPSPs
1053 (below). Scale bars for all traces are y = 10 mV (1mV), x = 20 ms (500 ms) for EPSPs (mEPSPs).
1054 **(E-G)** Quantification showing average mEPSP amplitude, EPSP amplitude, and NLS quantal
1055 content in pre-GAL4 control and pre-GAL4 driven *sra* RNAi in both the presence and absence of
1056 $GluRIIA^{SP16}$. *p<0.05, **p<0.01, ***p<0.001 by Student's T-test versus non-challenged genetic
1057 control.

1058

1059 **Figure 8.** Maintenance of presynaptic homeostatic potentiation is impaired by neuronal
1060 overexpression of *sra*, but acute expression is not. **(A-C)** Quantification showing average mEPSP
1061 amplitude, EPSP amplitude, and NLS quantal content in pre-GAL4 control and pre-GAL4 driven
1062 *sra* overexpression (OE). Black points show DMSO control synapses, while green points show
1063 synapses treated with PhTx. **(D, H)** Representative electrophysiological traces of EPSPs (above)
1064 and mEPSPs (below). Scale bars for all traces are y = 10 mV (1mV), x = 20 ms (500 ms) for EPSPs
1065 (mEPSPs). **(E-G)** Quantification showing average mEPSP amplitude, EPSP amplitude, and NLS
1066 quantal content in pre-GAL4 control and pre-GAL4 driven *sra* OE in both the presence and
1067 absence of $GluRIIA^{SP16}$. *p<0.05, **p<0.01, ***p<0.001 by Student's T-test versus non-
1068 challenged genetic control.

1069

1070 **Figure 9.** Pharmacological inhibition of calcineurin partially rescues the PHP deficit observed in
1071 chronically challenged postsynaptic overexpression of *sra* animals. **(A-C)** Quantification showing

1072 average mEPSP amplitude, EPSP amplitude, and NLS quantal content in post-GAL4 control and
1073 post-GAL4 driven *sra* overexpression (OE) in both the presence and absence of 50µM FK506.
1074 Black points show DMSO control synapses while dark pink points represent 50µM FK506. **(D)**
1075 Representative electrophysiological traces of EPSPs (above) and mEPSPs (below). Scale bars for
1076 all traces are y = 10 mV (1mV), x = 20 ms (500 ms) for EPSPs (mEPSPs). Two-way ANOVAs
1077 were used to compare each genotype with and without drug followed by a Tukey's HSD test for
1078 multiple comparisons. *p<0.05, **p<0.01, ***p<0.001.

1079

1080 **Figure 10.** Pharmacological inhibition of calcineurin rescues the PHP deficit observed in
1081 chronically challenged presynaptic knockdown of *sra* animals. **(A-C)** Quantification showing
1082 average mEPSP amplitude, EPSP amplitude, and NLS quantal content in pre-GAL4 control and
1083 pre-GAL4 driven *sra* knockdown in both the presence and absence of 50µM FK506. Black points
1084 show DMSO control synapses while dark pink points represent 50µM FK506. **(D)** Representative
1085 electrophysiological traces of EPSPs (above) and mEPSPs (below). Scale bars for all traces are y
1086 = 10 mV (1mV), x = 20 ms (500 ms) for EPSPs (mEPSPs). Two-way ANOVAs were used to
1087 compare each genotype with and without drug followed by a Tukey's HSD test for multiple
1088 comparisons. *p<0.05, **p<0.01, ***p<0.001.

1089

1090 **Figure 11.** Maintenance of presynaptic homeostatic potentiation can be further potentiated by
1091 pharmacologically inhibiting calcineurin. **(A-D)** Quantification showing average mEPSP
1092 amplitude, EPSP amplitude, NLS quantal content, and mEPSP frequency in wild type and
1093 *GluRIIA*^{SP16} animals. Black points show 10µM DMSO control, light pink points show 10µM
1094 FK506, grey points show 50µM DMSO control, and dark pink points show 50µM FK506. **(E,F)**
1095 Quantification of failure analysis experiment. 0.10mM Ca^{2+} was used in this experiment. "%
1096 failures" represents the number of stimulation pulses that failed to elicit any discernable response
1097 out of the 100 total pulses per synapse. Black points represent DMSO control, while the dark pink
1098 points represent 50µM FK506. **(G-I)** Quantification showing average mEPSP amplitude, EPSP
1099 amplitude, and NLS quantal content in wild type and *GluRIIA*^{SP16} animals dissected in low calcium
1100 conditions (0.20mM Ca^{2+}). Black points represent DMSO control, while the dark pink points

represent 50μM FK506. *p<0.05, **p<0.01, ***p<0.001 by Student's T-test versus non-drugged control.

Figure 12. Dual pre- and postsynaptic knockdown of *CaNB* does not block PHP while knockdown in muscle alone precluded the maintenance of PHP **(A-C)** Quantification showing average mEPSP amplitude, EPSP amplitude, and NLS quantal content in pre + post-GAL4 control and pre + post-GAL4 driven *CaNB* RNAi. Black points show DMSO control synapses, green points show synapses treated with PhTx, and magenta points show animals chronically challenged with *GluRIII* RNAi. **(D, H)** Representative electrophysiological traces of EPSPs (above) and mEPSPs (below). Scale bars for all traces are y = 10 mV (1mV), x = 20 ms (500 ms) for EPSPs (mEPSPs). **(E-G)** Quantification showing average mEPSP amplitude, EPSP amplitude, and NLS quantal content in post-GAL4 control and post-GAL4 driven *CaNB* knockdown. Black points show DMSO control synapses, green points show synapses treated with PhTx, and magenta points show animals chronically challenged with *GluRIII* RNAi. *p<0.05, **p<0.01, ***p<0.001 by Multiple Student's T-test and corrected for multiple comparisons using the Holm-Sidak method. DMSO controls were compared to PhTx and *GluRIII* RNAi synapses for driver controls and separately for *CaNB* RNAi.

Conflict of Interest

The authors declare that the research was conducted in the absence of any commercial or financial relationships that could be construed as a potential conflict of interest.

Author Contributions

NSA and CAF designed the research, analyzed the data, and wrote the manuscript. NSA performed the research. Both authors contributed to the article and approved the submitted version.

Funding

1127 This work was supported by grants from the National Institutes of Health/NINDS (NS085164 and
1128 NS130108) to CAF. This work was also supported by NIN/NINDS grant supplement to NSA for
1129 grant NS085164 (PI - CAF). Additional funds supporting parts of this work have been provided
1130 by the University of Iowa Carver College of Medicine (CCOM) and the PI's home department
1131 within CCOM, Anatomy and Cell Biology.

1132

1133 **Acknowledgements**

1134 We thank members of the Frank lab for helpful comments throughout this study. We thank the
1135 laboratories of Tina Tootle, Toshihiro Kitamoto, Pamela Geyer, and Lori Wallrath for helpful
1136 discussions. Additionally, we thank Drs. Samuel Young, Joshua Weiner, and Catherine
1137 Marcinkiewcz for helpful suggestions. We also thank the Bloomington Drosophila Resource Stock
1138 Center for several fly stocks detailed in the Methods section.

1139

1140 **Supplementary Material**

1141 Supplementary Tables S1-S4 and S7-S12 show raw electrophysiology data. Table S5 shows raw
1142 bouton counts and measurements for NMJ growth assessment. Table S6 shows raw pCaMKII and
1143 GluRIII intensity measurements.

1144

1145 **Data Availability Statement**

1146 The raw datasets for this study will be made available by the authors.

1147

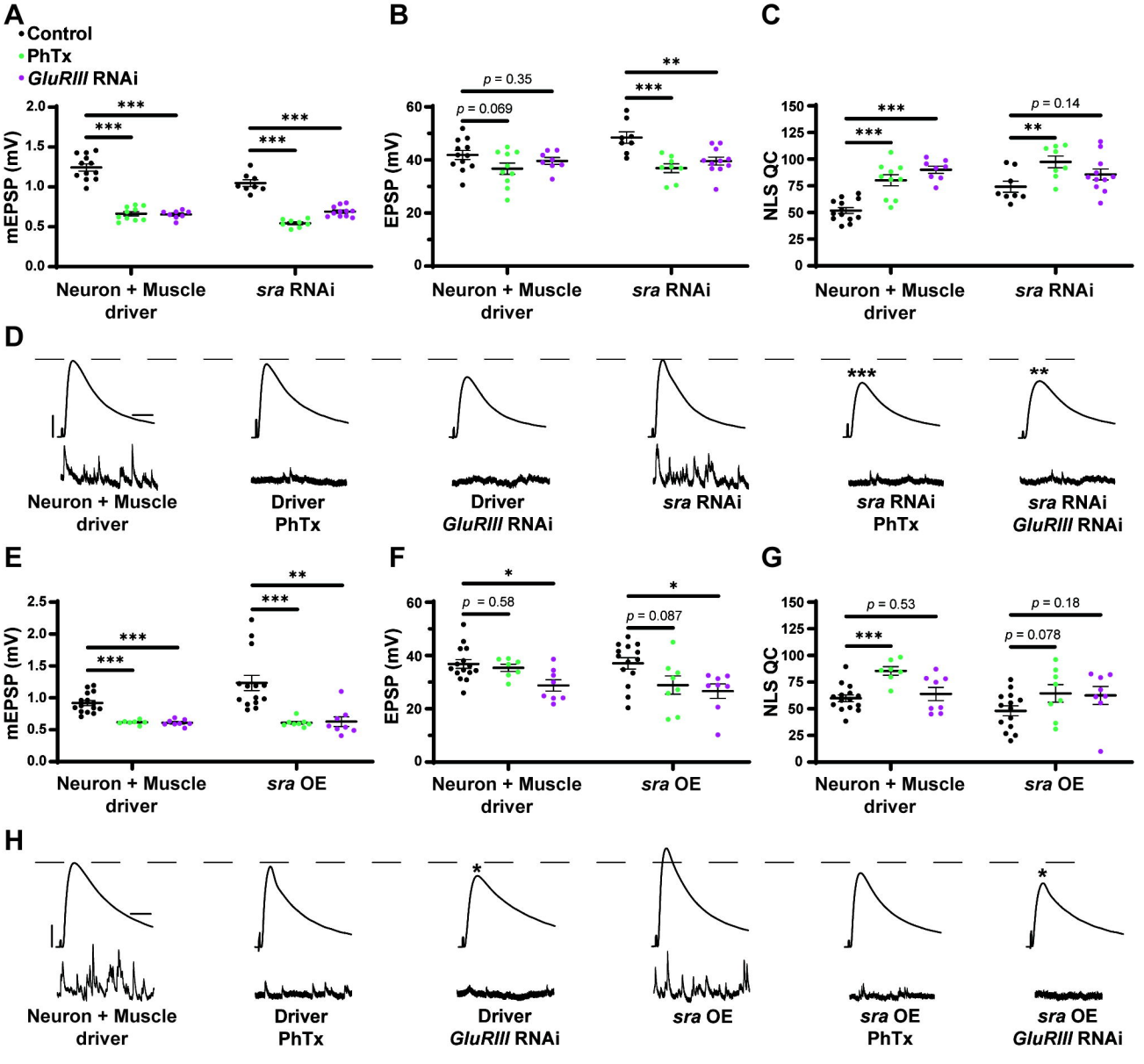
A
Control
PhTx
GluRIII RNAi
mEPSP (mV)
Neuron + Muscle driver
sra RNAi
B
EPSP (mV)
p = 0.35
p = 0.069
C
NLS QC
p = 0.14
D
Neuron + Muscle driver
Driver PhTx
Driver GluRIII RNAi
sra RNAi
sra RNAi PhTx
sra RNAi GluRIII RNAi
E
sra OE
F
p = 0.58
p = 0.087
G
p = 0.53
p = 0.078
H
Driver PhTx
Driver GluRIII RNAi
sra OE
sra OE PhTx
sra OE GluRIII RNAi

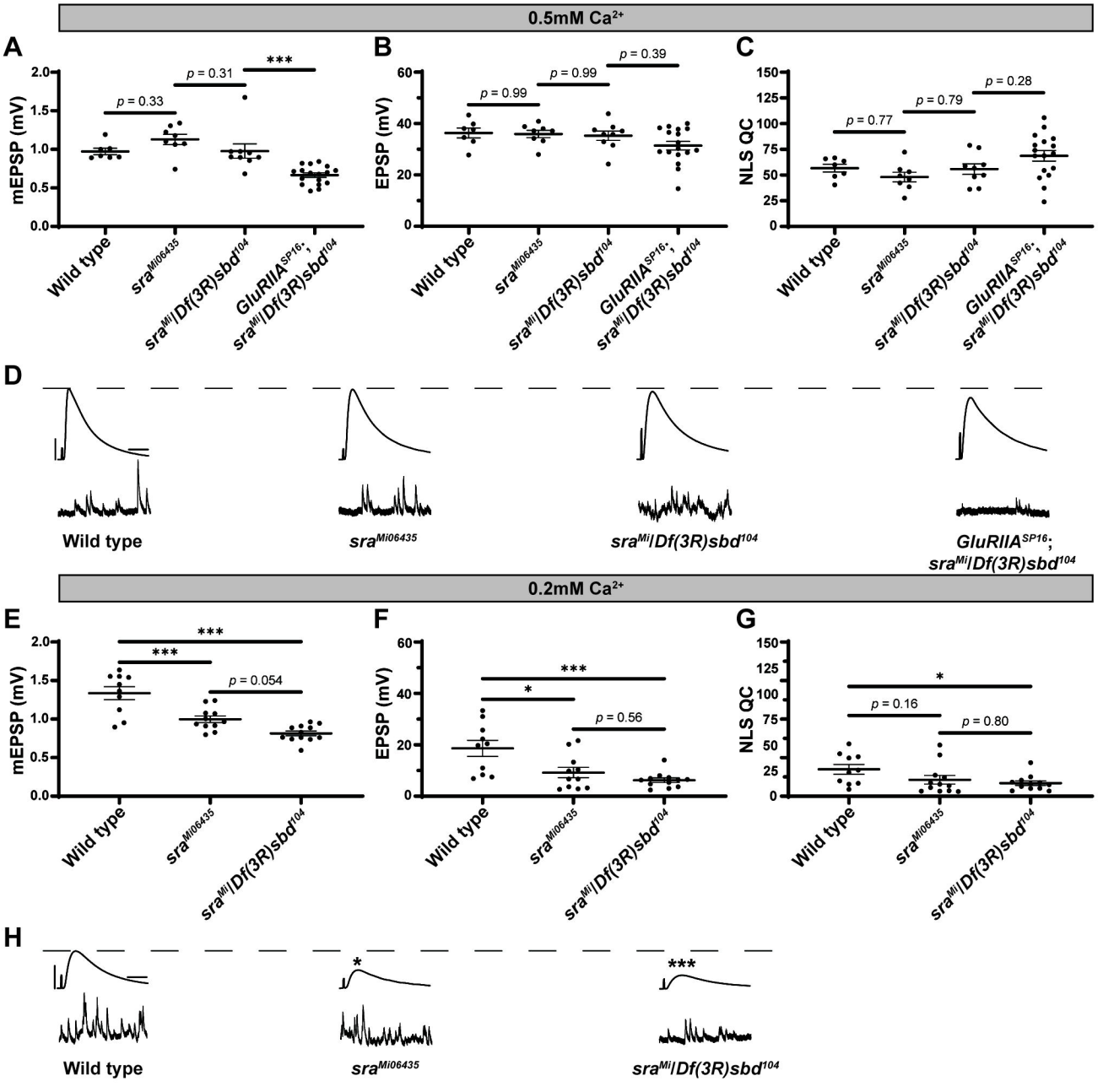
0.5mM Ca2+
A
mEPSP (mV)
p = 0.33
p = 0.31
***
Wild type
sraMi06435
sraMi/Df(3R)sbd104
GluRIIASP16; sraMi/Df(3R)sbd104
B
EPSP (mV)
p = 0.99
p = 0.99
p = 0.39
C
NLS QC
p = 0.77
p = 0.79
p = 0.28
D
Wild type
sraMi06435
sraMi/Df(3R)sbd104
GluRIIASP16; sraMi/Df(3R)sbd104
0.2mM Ca2+
E
mEPSP (mV)
***
***
p = 0.054
F
EPSP (mV)
***
*
p = 0.56
G
NLS QC
*
p = 0.16
p = 0.80
H
*
***
Wild type
sraMi06435
sraMi/Df(3R)sbd104

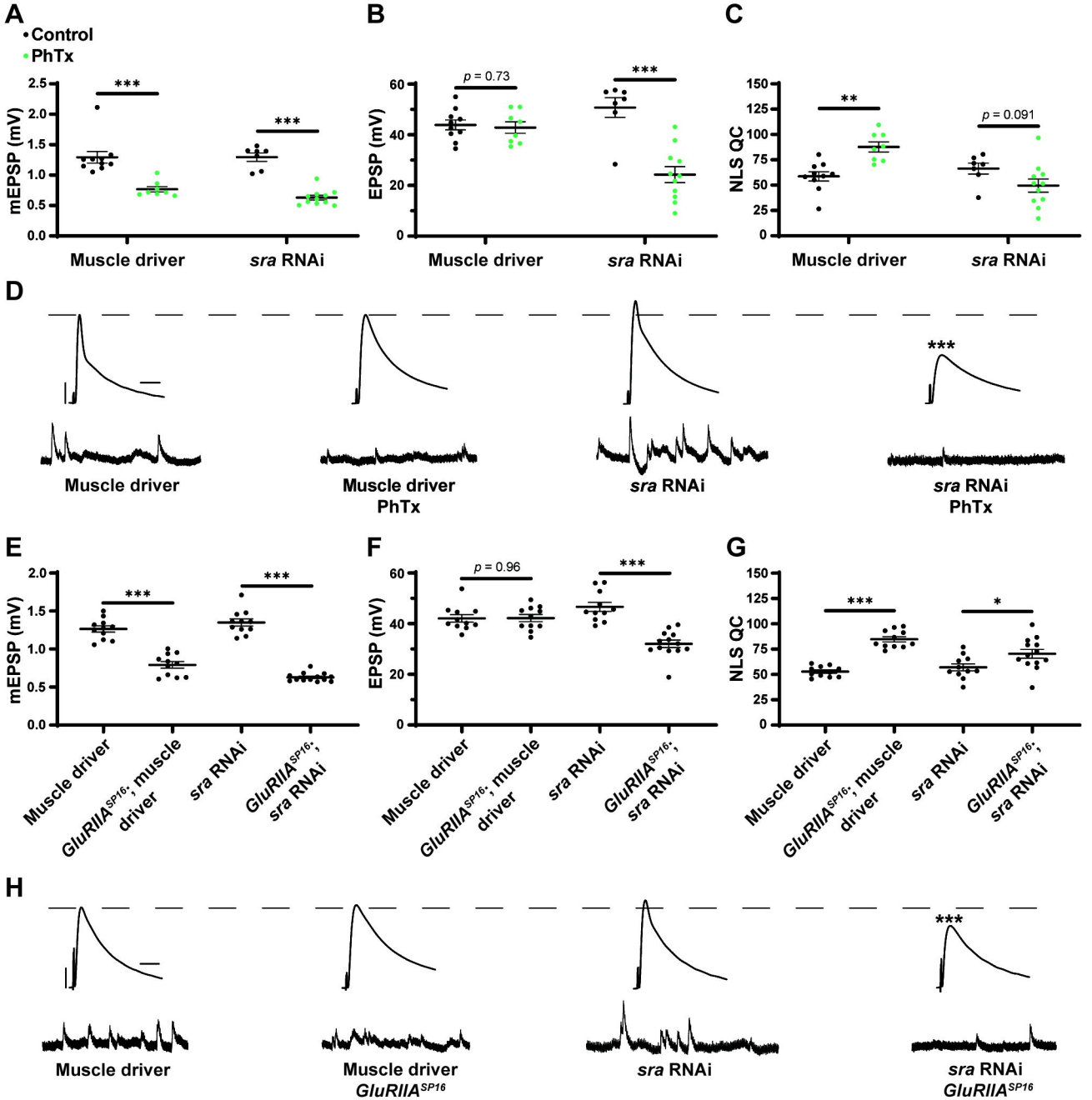
A
Control
PhTx
mEPSP (mV)
***
***
Muscle driver
sra RNAi
B
EPSP (mV)
p = 0.73
***
Muscle driver
sra RNAi
C
NLS QC
**
p = 0.091
Muscle driver
sra RNAi
D
***
Muscle driver
Muscle driver PhTx
sra RNAi
sra RNAi PhTx
E
mEPSP (mV)
***
***
Muscle driver
GluRIIA^SP16; muscle driver
sra RNAi
GluRIIA^SP16; sra RNAi
F
EPSP (mV)
p = 0.96
***
Muscle driver
GluRIIA^SP16; muscle driver
sra RNAi
GluRIIA^SP16; sra RNAi
G
NLS QC
***
*
Muscle driver
GluRIIA^SP16; muscle driver
sra RNAi
GluRIIA^SP16; sra RNAi
H
***
Muscle driver
Muscle driver GluRIIA^SP16
sra RNAi
sra RNAi GluRIIA^SP16

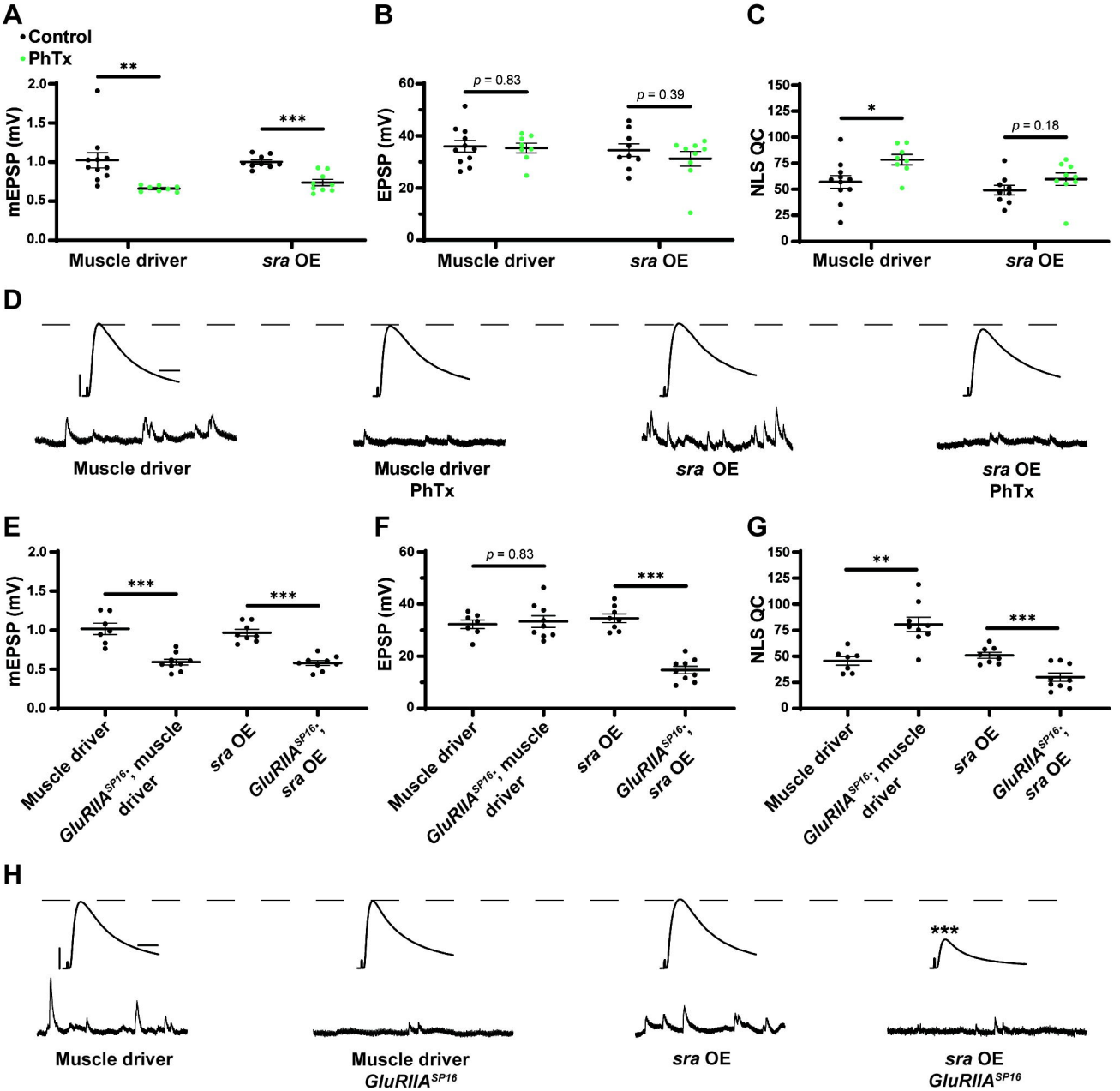
A
Control
PhTx
mEPSP (mV)
2.0
1.5
1.0
0.5
0.0
**
***
Muscle driver
sra OE
B
EPSP (mV)
60
40
20
0
p = 0.83
p = 0.39
Muscle driver
sra OE
C
NLS QC
150
125
100
75
50
25
0
*
p = 0.18
Muscle driver
sra OE
D
Muscle driver
Muscle driver PhTx
sra OE
sra OE PhTx
E
mEPSP (mV)
2.0
1.5
1.0
0.5
0.0
***
***
Muscle driver
GluRIIA^SP16; muscle driver
sra OE
GluRIIA^SP16; sra OE
F
EPSP (mV)
60
40
20
0
p = 0.83
***
Muscle driver
GluRIIA^SP16; muscle driver
sra OE
GluRIIA^SP16; sra OE
G
NLS QC
150
125
100
75
50
25
0
**
***
Muscle driver
GluRIIA^SP16; muscle driver
sra OE
GluRIIA^SP16; sra OE
H
***
Muscle driver
Muscle driver GluRIIA^SP16
sra OE
sra OE GluRIIA^SP16

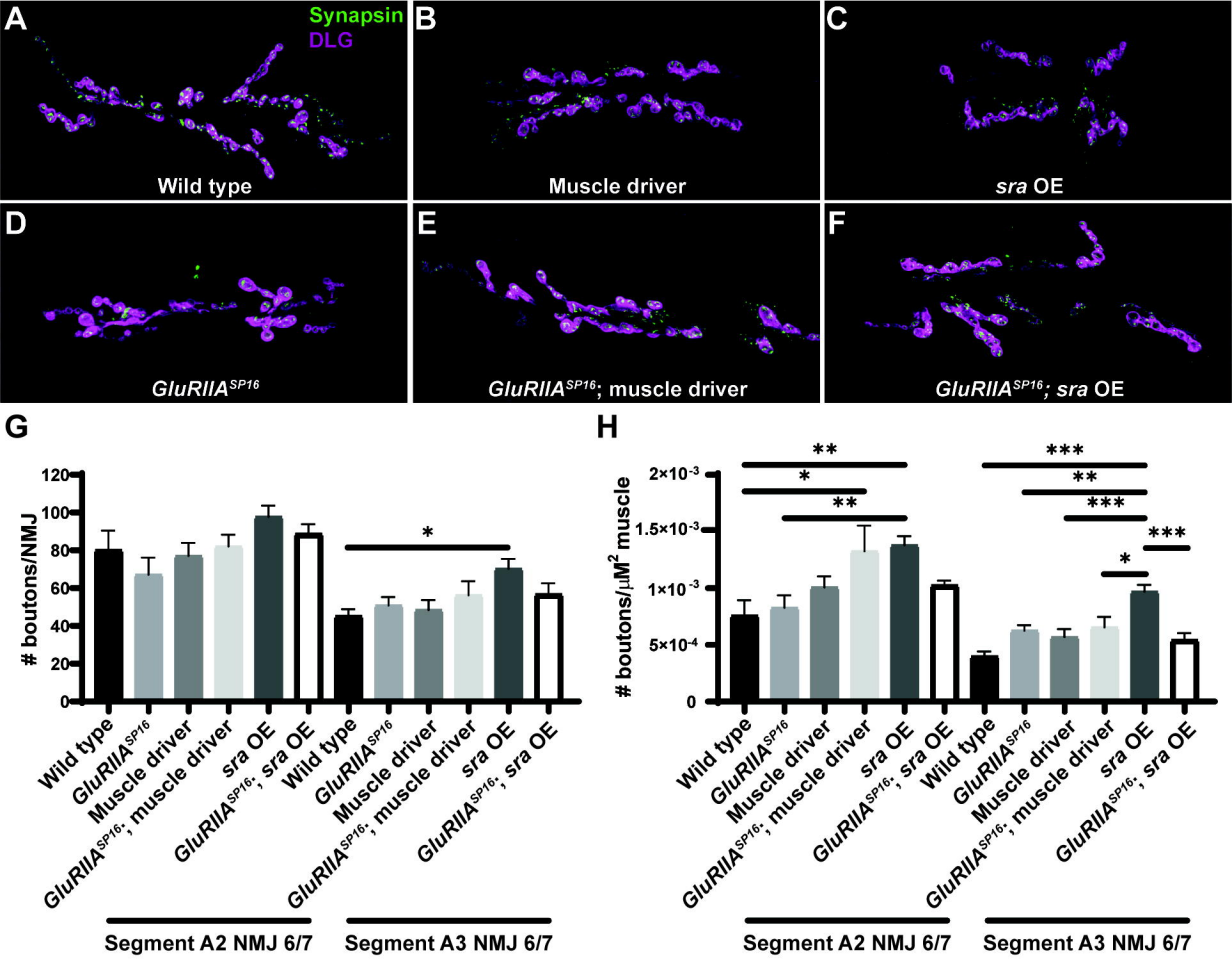
A
Synapsin
DLG
Wild type
B
Muscle driver
C
sra OE
D
GluRIIA^SP16
E
GluRIIA^SP16; muscle driver
F
GluRIIA^SP16; sra OE
G
boutons/NMJ
120
100
80
60
40
20
0
*
Wild type
GluRIIA^SP16
Muscle driver
GluRIIA^SP16; muscle driver
sra OE
GluRIIA^SP16; sra OE
Wild type
GluRIIA^SP16
Muscle driver
GluRIIA^SP16; muscle driver
sra OE
GluRIIA^SP16; sra OE
Segment A2 NMJ 6/7
Segment A3 NMJ 6/7
H
boutons/μM² muscle
2×10⁻³
1.5×10⁻³
1×10⁻³
5×10⁻⁴
0
**
*
**
***
**
***
*
***
Wild type
GluRIIA^SP16
Muscle driver
GluRIIA^SP16; muscle driver
sra OE
GluRIIA^SP16; sra OE
Wild type
GluRIIA^SP16
Muscle driver
GluRIIA^SP16; muscle driver
sra OE
GluRIIA^SP16; sra OE
Segment A2 NMJ 6/7
Segment A3 NMJ 6/7

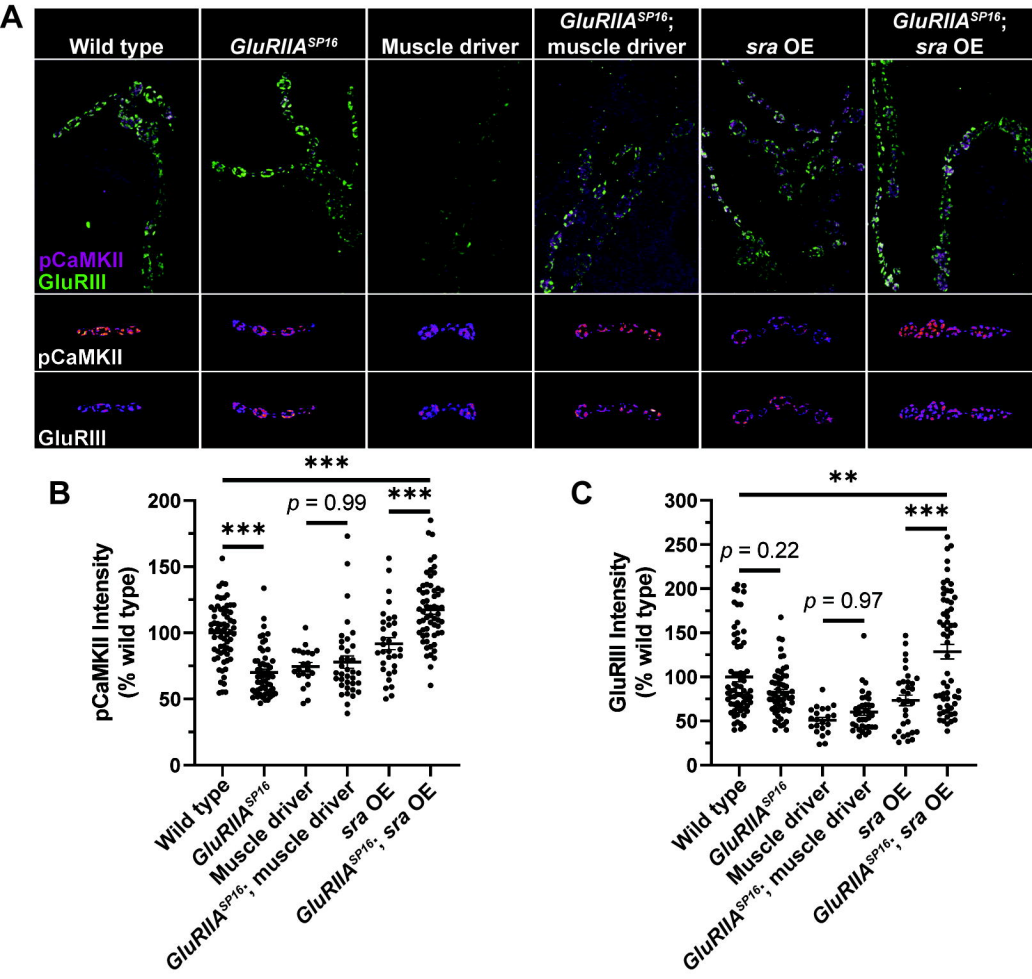
A
Wild type
GluRIIA^SP16
Muscle driver
GluRIIA^SP16; muscle driver
sra OE
GluRIIA^SP16; sra OE
pCaMKII
GluRIII
pCaMKII
GluRIII
B
pCaMKII Intensity (% wild type)
***
p = 0.99
***
***
C
GluRIII Intensity (% wild type)
**
p = 0.22
p = 0.97
***
Wild type
GluRIIA^SP16
Muscle driver
GluRIIA^SP16; muscle driver
sra OE
GluRIIA^SP16; sra OE

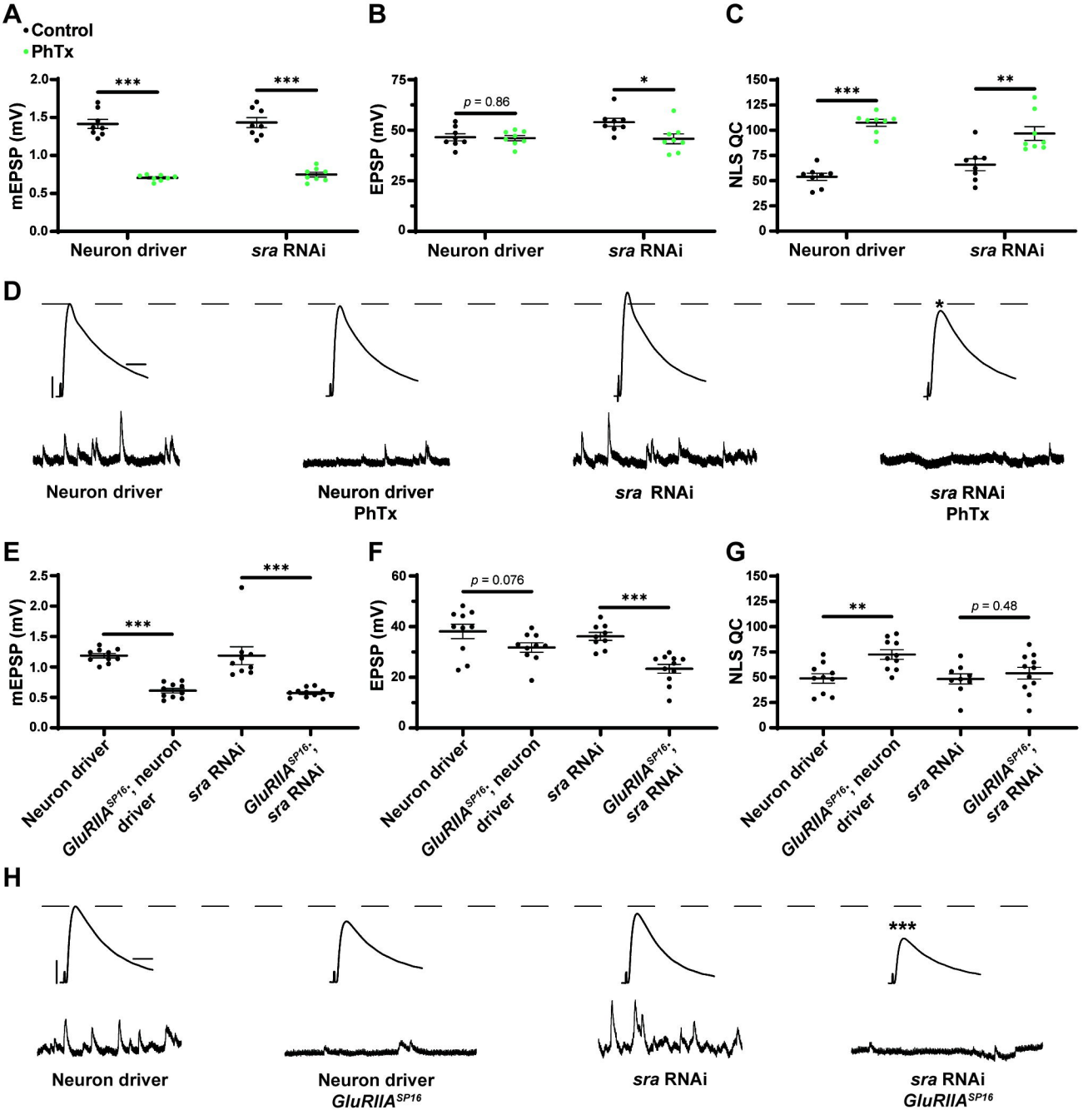
A
Control
PhTx
mEPSP (mV)
2.0
1.5
1.0
0.5
0.0
***
***
Neuron driver
sra RNAi
B
EPSP (mV)
75
50
25
0
p = 0.86
*
Neuron driver
sra RNAi
C
NLS QC
150
125
100
75
50
25
0
***
**
Neuron driver
sra RNAi
D
*
Neuron driver
Neuron driver PhTx
sra RNAi
sra RNAi PhTx
E
mEPSP (mV)
2.5
2.0
1.5
1.0
0.5
0.0
***
***
Neuron driver
GluRIIA^SP16; neuron driver
sra RNAi
GluRIIA^SP16; sra RNAi
F
EPSP (mV)
60
40
20
0
p = 0.076
***
Neuron driver
GluRIIA^SP16; neuron driver
sra RNAi
GluRIIA^SP16; sra RNAi
G
NLS QC
150
125
100
75
50
25
0
**
p = 0.48
Neuron driver
GluRIIA^SP16; neuron driver
sra RNAi
GluRIIA^SP16; sra RNAi
H
***
Neuron driver
Neuron driver GluRIIA^SP16
sra RNAi
sra RNAi GluRIIA^SP16

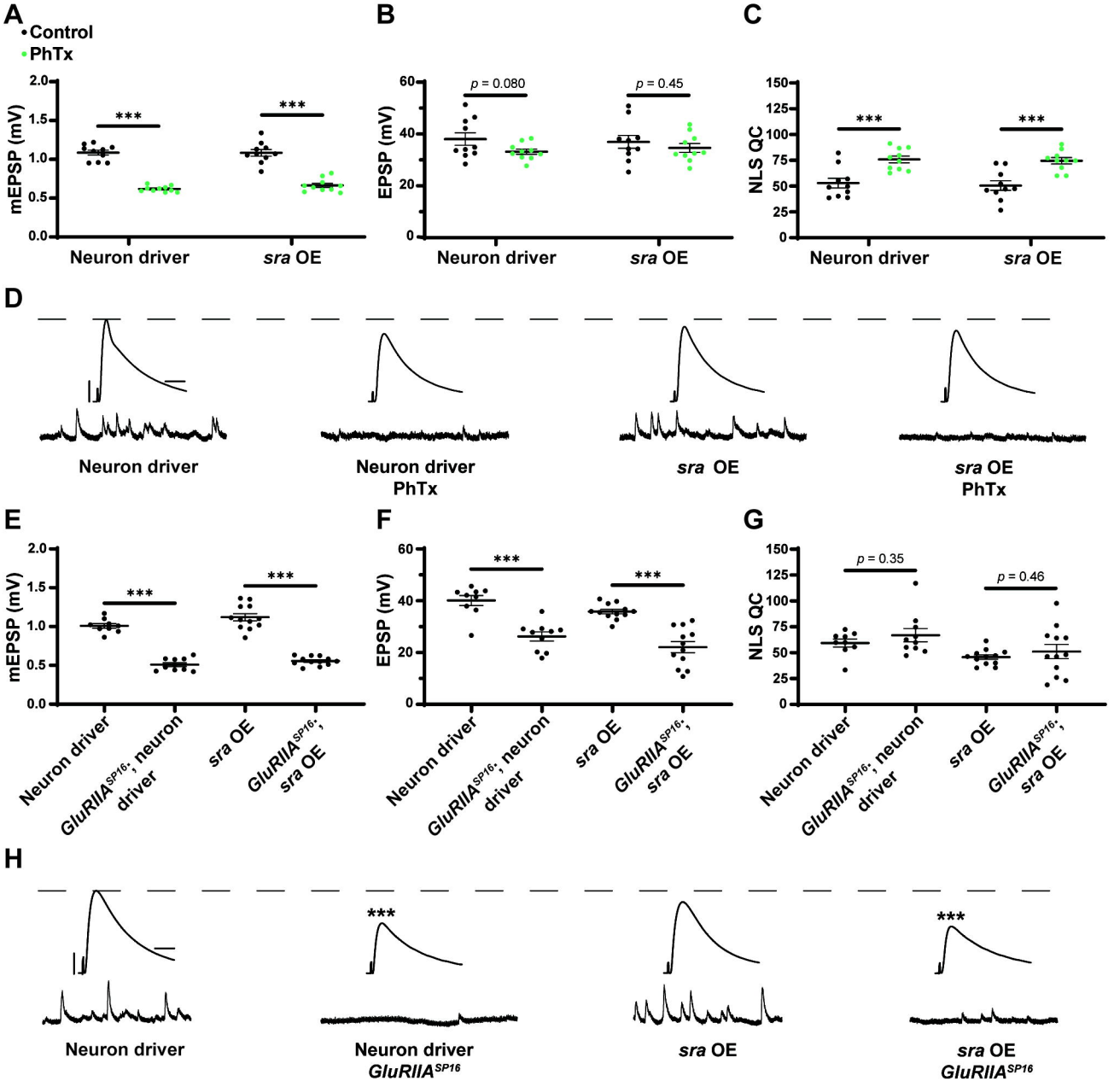
A
Control
PhTx
mEPSP (mV)
2.0
1.5
1.0
0.5
0.0
***
***
Neuron driver
sra OE
B
EPSP (mV)
60
40
20
0
p = 0.080
p = 0.45
Neuron driver
sra OE
C
NLS QC
150
125
100
75
50
25
0
***
***
Neuron driver
sra OE
D
Neuron driver
Neuron driver PhTx
sra OE
sra OE PhTx
E
mEPSP (mV)
2.0
1.5
1.0
0.5
0.0
***
***
Neuron driver
GluRIIA SP16, neuron driver
sra OE
GluRIIA SP16, sra OE
F
EPSP (mV)
60
40
20
0
***
***
Neuron driver
GluRIIA SP16, neuron driver
sra OE
GluRIIA SP16, sra OE
G
NLS QC
150
125
100
75
50
25
0
p = 0.35
p = 0.46
Neuron driver
GluRIIA SP16, neuron driver
sra OE
GluRIIA SP16, sra OE
H
***
***
Neuron driver
Neuron driver GluRIIA SP16
sra OE
sra OE GluRIIA SP16

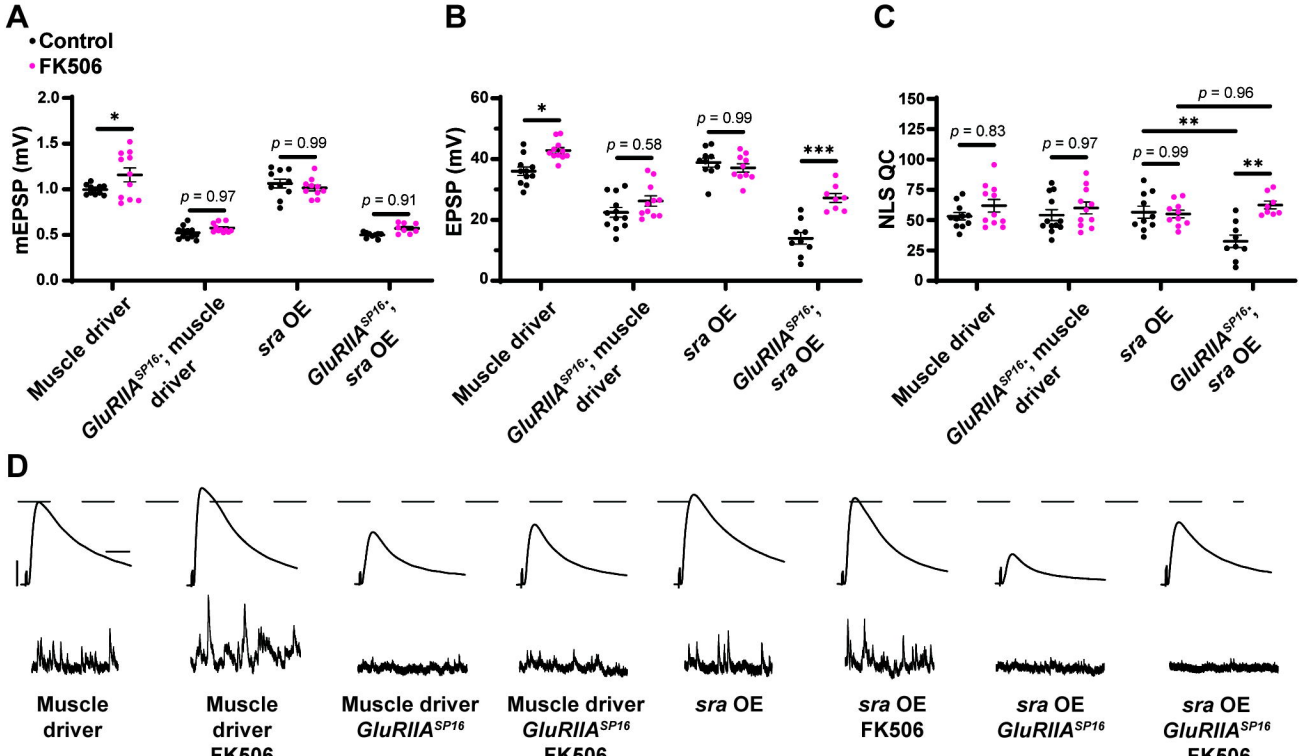
A
Control
FK506
mEPSP (mV)
2.0
1.5
1.0
0.5
0.0
*
p = 0.97
p = 0.99
p = 0.91
Muscle driver
GluRIIA^SP16/+; muscle driver
sra OE
GluRIIA^SP16/+; sra OE
B
EPSP (mV)
60
40
20
0
*
p = 0.58
p = 0.99
***
C
NLS QC
150
125
100
75
50
25
0
p = 0.83
p = 0.97
p = 0.99
p = 0.96
**
**
D
Muscle driver
Muscle driver FK506
Muscle driver GluRIIA^SP16
Muscle driver GluRIIA^SP16 FK506
sra OE
sra OE FK506
sra OE GluRIIA^SP16
sra OE GluRIIA^SP16 FK506

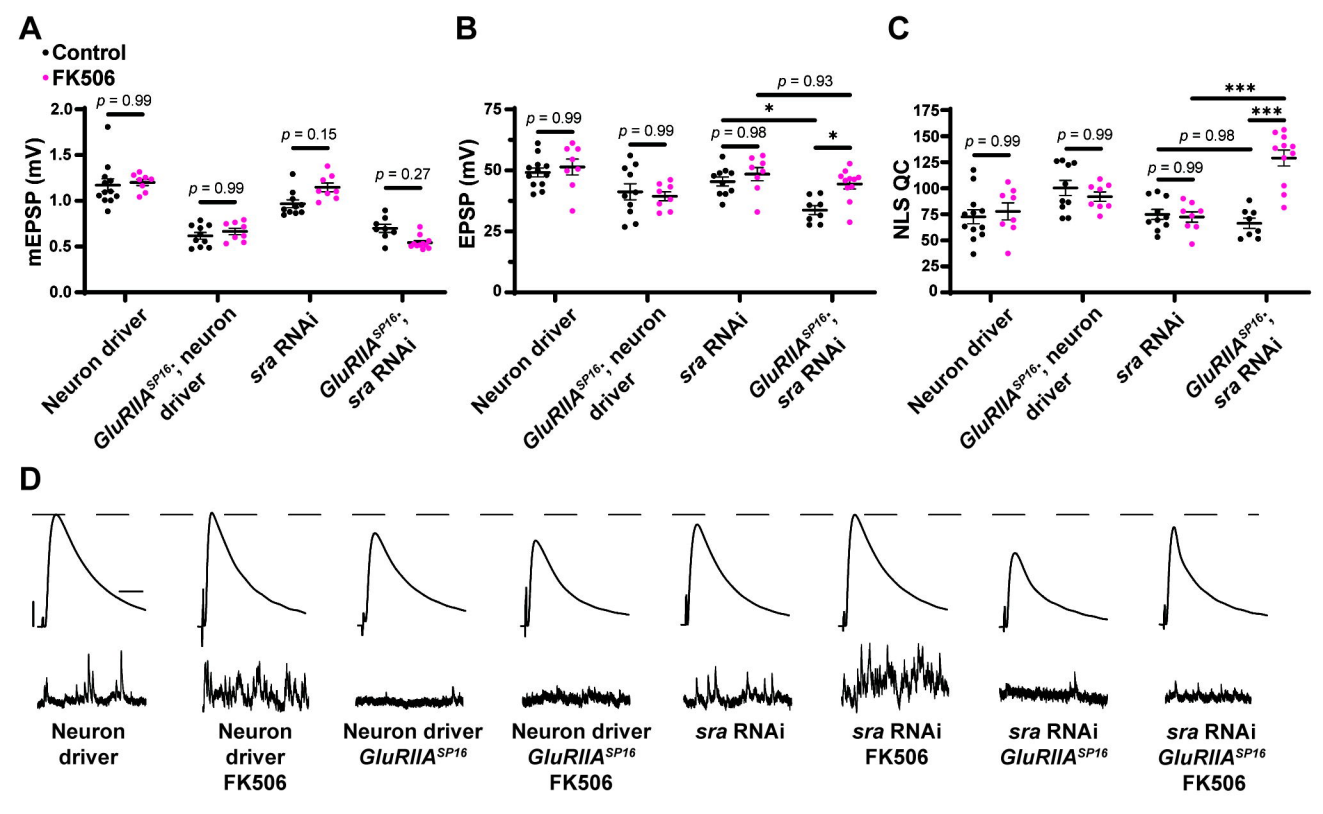
A
Control
FK506
mEPSP (mV)
p = 0.99
p = 0.99
p = 0.15
p = 0.27
Neuron driver
GluRIIA^SP16; neuron driver
sra RNAi
GluRIIA^SP16; sra RNAi
B
EPSP (mV)
p = 0.99
p = 0.99
p = 0.98
p = 0.93
*
*
C
NLS QC
p = 0.99
p = 0.99
p = 0.99
p = 0.98
***
***
D
Neuron driver
Neuron driver FK506
Neuron driver GluRIIA^SP16
Neuron driver GluRIIA^SP16 FK506
sra RNAi
sra RNAi FK506
sra RNAi GluRIIA^SP16
sra RNAi GluRIIA^SP16 FK506

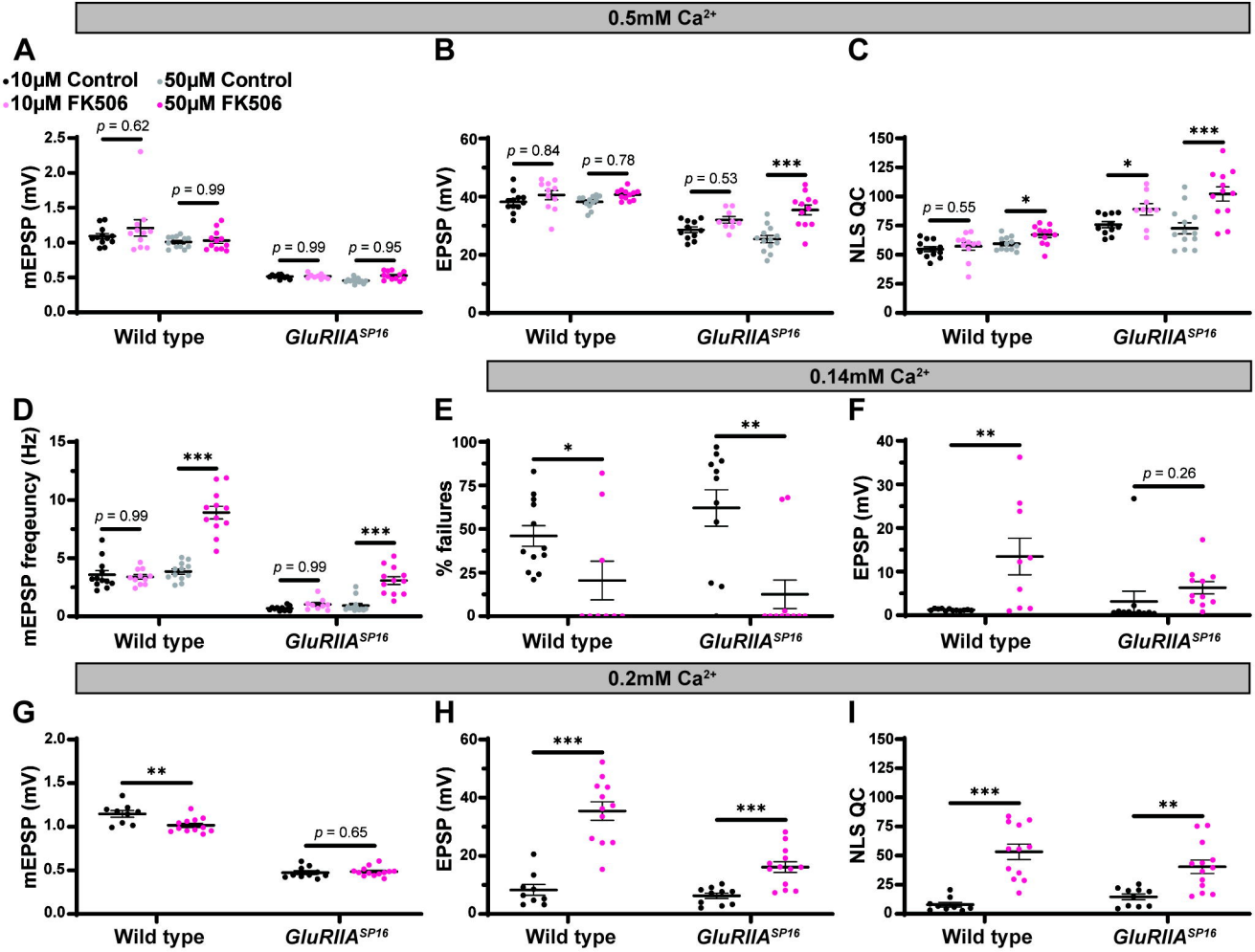
0.5mM Ca2+
A
B
C
10μM Control
50μM Control
10μM FK506
50μM FK506
mEPSP (mV)
EPSP (mV)
NLS QC
p = 0.62
p = 0.99
p = 0.99
p = 0.95
p = 0.84
p = 0.78
p = 0.53
***
p = 0.55
*
*
***
Wild type
GluRIIA SP16
0.14mM Ca2+
D
E
F
mEPSP freqeuncy (Hz)
% failures
EPSP (mV)
p = 0.99
***
p = 0.99
***
*
**
**
p = 0.26
Wild type
GluRIIA SP16
0.2mM Ca2+
G
H
I
mEPSP (mV)
EPSP (mV)
NLS QC
**
p = 0.65
***
***
***
**
Wild type
GluRIIA SP16

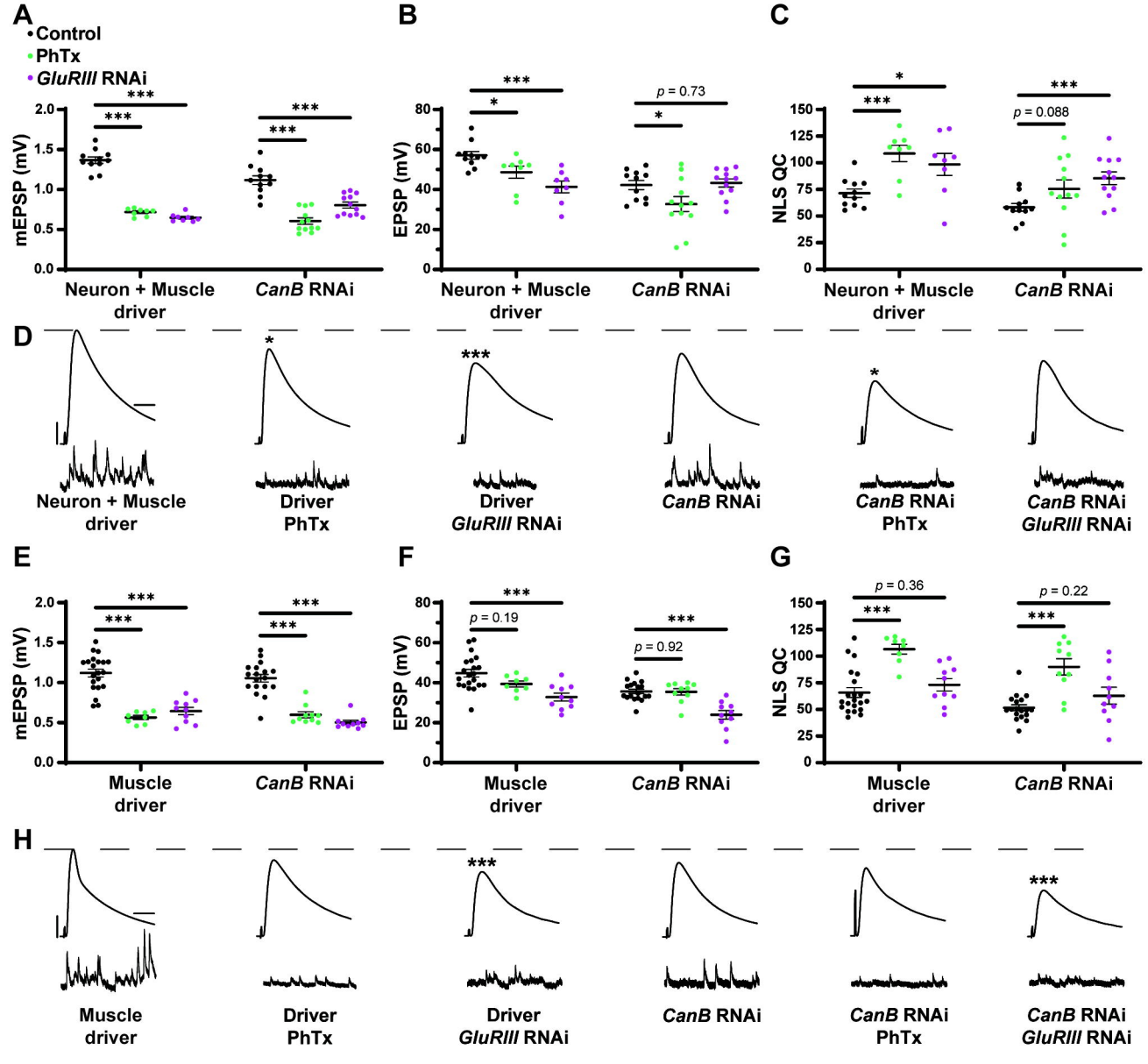
A
Control
PhTx
GluRIII RNAi
mEPSP (mV)
Neuron + Muscle driver
CanB RNAi
B
EPSP (mV)
p = 0.73
C
NLS QC
p = 0.088
D
Neuron + Muscle driver
Driver PhTx
Driver GluRIII RNAi
CanB RNAi
CanB RNAi PhTx
CanB RNAi GluRIII RNAi
E
Muscle driver
F
p = 0.19
p = 0.92
G
p = 0.36
p = 0.22
H